



ADVANCED MASTERS IN STRUCTURAL ANALYSIS  
OF MONUMENTS AND HISTORICAL CONSTRUCTIONS



# Master's Thesis

Iat Meng Wan

## **Marco Modeling of Ruins of St. Paul's, Macau**

This Masters Course has been funded with support from the European Commission. This publication reflects the views only of the author, and the Commission cannot be held responsible for any use which may be made of the information contained therein.



## **ACKNOWLEDGEMENT**

This work was performed under direct supervision of Dr. Jan Zeman of Czech Technical University in Prague and I am grateful to his fruitful discussion and encouragement during my stay in Czech Republic.

The financial support from Erasmus Mundus Program of European Commission is greatly acknowledged.

I would like to have special thanks to Prof. Iu of University of Macau for making me possible to come to Europe to study and work in University of Minho, Portugal and Czech Technical University in Prague, Czech Republic respectively. I would also like to thank, Mr. Angus Lam of Department of Civil and Environmental Engineering of University of Macau for his interesting discussions.

Finally, I would like to thank all my family, for their love and support.



## **ABSTRACT**

Modeling of historic masonry structure requires specific strategies. There are three different types of modeling approach, namely, detailed micro-modeling, simplified micro-modeling and macro-modeling. Choice of the approach depends on the complexity of structure, time and cost. In the present study, a parametric stress analysis of façade of the Ruins of St Paul's in Macau is carried out. The adopted modeling approach is based on the uncoupled homogenization strategy, where the effective elastic properties are first estimated using an engineering homogenization technique followed by a macroscopic two-dimensional analysis of the structure. This approach is conceptually simple. Linear elastic finite element analysis is carried out to study the in plane stresses due to self weight of the structure. An effective mesh size of 25,000 is found to be enough for finite element meshing. Stress analysis shows that the maximum stress ranges from 0.21 MPa (tension) to -0.22 MPa (compression). Critical points regarding high compressive and tensile stress are detected, indicating the possible locations for repair checking and strengthening.



## **ABSTRAKT**

Modelování historických zděných konstrukcí vyžaduje specifické přístupy. Celkově lze rozlišit tři základní typy, jmenovitě podrobné mikromodelování, zjednodušené mikromodelování a makromodelování. Volba vhodného přístupu závisí na složitosti konstrukce, dostupném času a finančních prostředcích. V rámci předkládané studie je provedena parametrická analýza rozložení napětí ve fasádě ruin Sv. Pavla v Macau. Zvolený modelovací přístup je založen na nesdružené homogenizační strategii, kde jsou nejprve určeny efektivní vlastnosti pomocí inženýrské homogenizace a následně provedena makroskopická dvojrozměrná analýza konstrukce. Výhodou tohoto přístupu je jeho koncepční jednoduchost. Konkrétně je provedena lineárně pružný výpočet pro zatížení vlastní tíhou za předpokladů rovinné napjatosti. Je prokázáno, že síť s 25,000 konečnými prvky je dostatečně přesná. Analýza napětí v konstrukci prokazuje rozsah napětí od 0.21 MPa (tah) do -0.22 MPa (tlak). Výpočet též identifikoval body vyznačující se zvýšenými hodnotami tlakových a tahových napětí, které zasluhují zvýšenou pozornost při monitorování a případných opravách konstrukce.



# CONTENTS

Chapter one: Introduction.....	1
1.1 Importance of computational modeling of masonry structures.....	1
1.2 Objectives and scope of the study.....	3
Chapter two: Modeling masonry.....	5
2.1 Modeling strategies.....	5
2.2 Material modeling.....	5
2.3 Micro modeling.....	6
2.4 Homogenization.....	7
2.5 Macro modeling.....	7
Chapter three: Historic perspective of the Ruins of St. Paul’s, Macau.....	9
3.1 History and importance.....	9
3.2 Intervention.....	10
Chapter four: Modeling of the Ruins of St. Paul’s, Macau.....	11
4.1 Finite element method.....	11
4.2 Material property of the Ruins of St. Paul’s, Macau.....	11
4.2.1 Granite.....	11
4.2.2 Mortar.....	12
4.3 Modeling of the structure.....	12
4.3.1 Linear elastic analysis.....	12
4.3.2 Analysis procedure.....	13
4.3.3 Homogenization of wall panel.....	15
4.4 Analysis and parametric study of the wall panel.....	18
4.4.1 General.....	18
4.4.2 Mesh study of the wall panel.....	19
4.4.3 Effects of elastic modulus.....	20

4.5	Analysis of the two dimensional plane of façade.....	20
4.5.1	General.....	20
4.5.2	Mesh study of the façade.....	21
4.5.3	Discussion of finite element results of the façade.....	22
	Chapter five: Conclusions.....	73
	References.....	75

## CHAPTER 1 INTRODUCTION

### 1.1 Importance of computational modeling of masonry structures

For architectural heritage, masonry structure is the most common type because of its simplicity, aesthetics, solidity and durability. Laying pieces of stone or bricks on top of each other, either with or without mortar, is a successful technique which has been used for thousands of year.

The analysis of historical masonry structures is a complex task. The understandings of mechanical behaviour of masonry through various types of approaches including non-destructive tests, laboratory investigation and computational analysis, are limited. Second, the use of existing knowledge is still not mature for the analysis of historic structures. Typical problems of the historic structures are (Lourenco, 2002)

- Geometric data is missing;
- Information about the inner core of the mechanical properties of the material used is difficult to obtain and expensive;
- There is large variability of mechanical properties, because of workmanship and the use of natural materials;
- Significant changes have occurred in the core and constitution of structural elements, associated with long construction periods;
- The construction sequence is unknown;
- Existing damage in the structure is unknown;
- Regulations and codes are not applicable.

The conservation and restoration of architecture heritage requires an updated and innovative technology that gradually deviates from traditional practice. Modern principles of intervention are referred to removability, minimum repair, respect of original design, safety, material compatibility and cost. The consideration of all these

aspect is challenging job, for which advanced knowledge of engineering analysis is necessary. Several methods and computational tools are available for the assessment of the mechanical properties of historic structures. It should be noted that different method will give different result, but there is no sufficient reason to prefer one method over another.

Advanced modeling of historic structure involves three main types of model, namely, structural component models, finite element models and discontinuum structural models. The structural component model approximates the actual geometry by using various types of structural elements such as beam, panel, truss, plate and shell elements. However, in many cases, it is difficult to represent the historic structures in terms of structural component model because of complex geometry. Two-dimensional and three-dimensional finite elements models are then necessary. In fact, historic structures always involve massive structural parts such as piers and buttresses, combined with large span arches and vaults. Finite element model can focus on the partial study of structural parts in the historical buildings, allowing the prediction of mechanical behaviour locally. Lastly, for particular type of historic structures, which are subjected to state of stress and strain that are highly heterogeneous, discontinuum models are required for analysis. For this type of models, the mechanical properties of mortar, masonry unit and unit-mortar interface are important parameters for analysis.

The results from computational modeling are important for understanding the behaviour of the structures. Potential damages may be detected from the interpretation of the results. Choice of numerical tools is therefore crucial step because time and cost are controlling factors. Simplicity over complexity is always the rule for analyzing the historical structures.

## 1.2 Objectives and scope of the study

This study focuses on the fundamental understanding of computational modeling for historical masonry structures. The primary aim of this study is the overview and evaluation of the numerical tools for analysis of one type of historical ruins structure. The application of the selected numerical tool is then demonstrated using a representative structure – The Ruins of St. Paul's in Macau.

The objectives of this study are

- To review the available numerical tools which are robust and accurate for modeling of the structure in question
- To select appropriate numerical tools, namely, macro-modeling, for analysis of one type of ruin structure
- To discuss the adequacy of the macro-modeling approach, in which the composite masonry material is idealized as continuum
- To discuss the suitability of the application of homogenization techniques to numerical modeling of ruin structure

Chapter 2 characterizes the modeling strategies and overviews the available numerical tools for modeling historical masonry structures. The tools include micro modeling, homogenization and macro modeling. The material modeling for masonry is also presented.

Chapter 3 introduces the historical perspective of The Ruins of St. Paul's, Macau. The history and importance of this architectural heritage is presented. The introduction of intervention of this ruin structure is then given.

Chapter 4 deals with marco modeling of The Ruins St. Paul's, Macau. Two dimensional linear elastic finite element analysis of the structure is presented. Homogenization technique is then applied to a panel of this ruin structure for parametric study.

Chapter 5 presents the final conclusions which can be derived from this study.



## **CHAPTER 2 MODELING MASONRY**

### **2.1 Modeling Strategies**

Masonry is a composite material showing directional properties which are typically zone of weakness. Lourenco (2002) mentioned that the numerical representation may focus on the macro-modeling of masonry as a continuum or the micro modeling of individual components like brick, block etc and mortar. It is then possible to apply the following strategies.

- Detailed micro-modeling – units and mortar are represented by continuum element whereas the unit-mortar interface is represented by discontinuum elements
- Simplified micro-modeling – the units become expanded and represented by continuum elements whereas the behaviour of the mortar joints and unit-mortar interface is lumped in discontinuum elements
- Macro-modeling – units, mortar and unit-mortar interface are smeared out in a homogenous continuum

In the first approach, Young's modulus and Poisson's ratio of unit and mortar are taken into account. The interface is represented by a slip surface with initial dummy stiffness. The interaction between unit, interface and mortar can be well studied. In the second approach, each joint, consisting of mortar and the two unit-interfaces, is represented by an average interface while the units are expanded to keep the geometry unchanged. Masonry is then regarded as a set of blocks bonded by slip lines at the joints. The third approach treats masonry as homogenous anisotropic continuum.

### **2.2 Material Modeling**

Masonry is heterogeneous material that consists of units and joints. Because of variation in material for joints and units, the modeling for masonry material is not simple task. The only common feature for all masonry material is its low tensile strength.

Therefore, accurate micro and macro modeling requires thorough experimental description of their material. As pointed out by Lourenco (1996), one of the most important features for material modeling is softening. He noted that “softening is gradual decrease of mechanical resistance under a continuous increase of deformation forced upon a material specimen or structure.” The behavior of softening for tensile failure has been studied by Hordijk (1991). For compressive failure, Vonk (1992) carried out test on concrete specimen and found out that the behavior in uniaxial compression is controlled by fracturing processes.

Depending on the complexity of the analysis, there are two major categories for material modeling. The first one is the group of closed-form constitutive laws (Pande et al., 1989; Lourenco et al., 1997; Papa and Nappi, 1997). In the second group, individual constituent is well studied and it is endowed with specific geometry and boundary material properties (Hart et al, 1998; Lourenco and Rots, 1997; Giambanco et al., 2001)

### **2.3 Micro Modeling**

Lourenco (1996) pointed out that an accurate micro-modeling must include all the basic types of failure mechanisms of masonry such as (a) cracking of the joints (b) sliding along the bed or head joints at low values of normal stress (c) cracking of the units in direct tension (d) diagonal tensile cracking of the units (e) “masonry crushing” He used the interface failure criterion to carry out the micro modeling for masonry. Details about the development of the model can be referred to Lourenco (1996).

He also suggested one simplified micro-modeling method in which the units are expanded in both directions by the mortar thickness and mortar joints are modeled with zero-thickness interface elements. Under this approach, the elastic properties of unit remain unchanged. The elastic stiffness (normal and shear) is then estimated as

$$k_n = \frac{E_u E_m}{h_m (E_u - E_m)}$$

$$k_s = \frac{G_u G_m}{h_m (G_u - G_m)}$$

Where  $E_u$  and  $E_m$  are the Young's moduli,  $G_u$  and  $G_m$  are the shear moduli, respectively for unit and mortar and  $h_m$  is the actual thickness of the joint.

## 2.4 Homogenization

The use of homogenization is a technique of computing a constitutive “relation between averages”, normally expressed by volume averaged field variable. Therefore, the structure size should be sufficiently larger than the size of the inhomogeneities. For carrying out the homogenization, a “representative volume element” must be selected so that its size is big enough to represent the “average” field variable.

Masonry is composite material and the homogenization technique becomes a popular tool for studying masonry recently (Cecchi & Di Marco, 2000; Cecchi & Sab 2002; Mistler et al, 2007). This method permits to establish constitutive relations in terms of average stresses and strains from the constitutive relations of the individual components.

In Anthoine's study (1995), the homogenization theory for periodic structure is applied to the analysis of the basic cell. Other authors, Pande et al. (1989); Papa (1990) and Pietruszczak and Niu (1992), have applied the homogenization in approximate manner.

## 2.5 Macro Modeling

The analysis of masonry structures can be performed with macro modeling if the number of units and joints are huge. For macro modeling, the stresses and strains will be determined on an average basis. Simple constitutive behaviour such as Mohr-Coulomb criterion, can be used as preliminary study. However, for a more advanced model, the

anisotropy arising from arrangement of unit and mortar must be considered. Hill (1948), Hoffman (1967) and Tsai and Wu (1971) proposed the anisotropic constitutive model from theoretical point of view. Later, De Borst and Feenstra (1990) and Schellekens and De Borst (1990) investigated this type of model through numerical calculation by implementing elastic-perfectly-plastic Hill yield criterion and elastic-perfectly-plastic Hoffman yield criterion respectively. Lourenco (1996) proposed a new model, namely, anisotropic plasticity model to study the behaviour of masonry. The yield criterion for tension and compression are considered separately, according to different failure mechanism. The former one is related to the localized fracture process usually showing the signs of cracking of the material. The latter one is associated with more distributed fracture process showing the crushing phenomenon of material.

## **CHAPTER THREE: HISTORICAL PERSPECTIVE OF THE RUINS OF ST. PAUL'S, MACAU**

### **3.1 History and Importance**

The **Ruins of St. Paul's** (Portuguese: *Ruínas de São Paulo*) refer to the façade of what was originally the **Cathedral of St. Paul**, a 17th century Portuguese cathedral in Macau dedicated to Saint Paul the Apostle. It was built from 1582 to 1602 by the Jesuits, the cathedral was the largest Catholic church in Asia at the time. It was also the first European University in South East Asia. An adjoining church was dedicated to the Mother of God in 1602, as stated in an inscribed stone that is laid on the side of façade. The church walls were built in taipa (chunam). Each nave divide included four heavy pillars. The only stone elements of the church were three arches in the interior and the granite façade itself which was finished in 1644.

In January 1835, a fierce fire burnt the church to the ground. Only the façade remained, together with parts of the taipa walls and the side of the bell tower adjoining the church. This was brought down shortly because of potential collapse problems. Subsequently three choir windows were inlaid with brick arches and the remains of the church was kept in use. The ground, previously as nave, was used as cemetery.

The ruins now consist of the southern stone façade — intricately carved between 1620 and 1627 by Japanese Christians in exile from their homeland and local craftsmen under the direction of Italian Jesuit Carlo Spinola — and the crypts of the Jesuits who established and maintained the Cathedral. The façade sits on a small hill, with 66 stone steps leading up to it. The carvings include Jesuit images with Oriental themes, such as a woman stepping on a seven-headed hydra, described by Chinese characters as 'the Holy Mother tramples the heads of the dragon'. A few of the other carvings are the

founders of the Jesuit Order, the conquest of Death by Jesus, and at the very top, a dove with wings outstretched.

Today, the ruins are one of Macau's most famous landmarks. In 2005, the Ruins of St. Paul were officially enlisted as part of the UNESCO World Heritage Site Historic Center of Macau. The role of the façade of St. Paul Ruin as a symbol of the culture and heritage of Macau is assured. Not only the monument is good example of inter-cultural design and craftsmanship but also bears in itself the memory and testimony of rich history of “West Meets East”.

### **3.2 Intervention**

The ruins were excavated and turned into the museum from 1990 to 1995 by the Cultural Institute of Macau and Macau Government. This process of changing the ruins into museum, namely, “musealization”, includes the following steps

- a) To cover or to protect significantly the revealed foundations after the excavation
- b) To make clear the history of the site by signaling existing element and clarifying their role
- c) To present the referred reconstitution – models, drawings and descriptions
- d) To establish a visiting circuit that allows the public to explore: to climb on the catwalk, to watch the area of the naves fro above, to imagine the once existing architecture, to look at the town from façade windows etc.
- e) To create museum spaces for visit
- f) To create security conditions through the uses of walls, grids and alarm systems

The facade is now buttressed with concrete and steel in a way which preserves the aesthetic integrity of the facade. A steel stairway allows tourists to climb up to the top of the facade from the rear.

## **CHAPTER 4 MODELING OF THE RUINS OF THE ST. PAUL'S, MACAU**

### **4.1 Finite Element Method**

The finite element method is the engineer's implementation of a thoroughly formal mathematical theory for constructing approximate solutions to partial differential equations occurring throughout engineering mechanics and physics. This implementation ultimately employs subdivision of the problem domain (geometry) into a finite number of small regions called finite elements. Many convenient shapes are available, such as triangles and quadrilaterals in two dimensions; and tetrahedra, pentahedra, and hexahedra for three dimensions. All combinations of appropriate boundary conditions become naturally included in the process. This basic constraint produces a set of algebraic equations, written on each finite element, which are then collected together using a procedure called "assembly" to form the global matrix statement. The approximation-dependent variable distribution is then determined through solution of this matrix statement using any linear algebra technique.

From the engineering aspect, the finite element analysis originated as the displacement method of the matrix structural analysis, which emerged over the course of several decades in research as a variant suitable for computers. By then, the key concepts of stiffness matrix and element assembly existed essentially in the form used today.

### **4.2 Material properties of the Ruins of the St. Paul**

#### **4.2.1 Granite**

The whole façade was constructed mainly with granite. Granite is a common and widely occurring type of igneous rock. Granite has a medium to coarse texture, occasionally with some individual crystals larger than the groundmass. This kind of rock can be pink

to dark gray or even black in color, depending on their chemistry and mineralogy. It is nearly always massive, hard and tough, and therefore it has gained widespread use as a construction stone. The average density of granite is  $2750 \text{ Kg/m}^3$ . Unlike concrete or steel, granite is a type of igneous rock that is rich in quartz and feldspar, the materials properties varies in a range. The Young's modulus of granite ranges from 53 to 70GPa and the Poisson's ratio is about 0.25.

#### **4.2.2 Mortar**

Another material was the mortar that was used to bind the granite block. Mortar is usually a mixture of sand, a binder such as cement or lime, and water and is applied as a paste which then sets hard. However, since this is a mixture, the exact properties of the mortar used in constructing the façade are not easily estimated as illustrated on selected data available in the literature. Therefore, the values of Young's modulus and Poisson ratio have been reviewed. The density ranges from 1540 to  $2400 \text{ Kg/m}^3$ . The Young's modulus for mortar ranges from 32.5 to 40GPa with Poisson's ratio of around 0.15 to 0.23 (Yurtdas et al. (2004)). According to Mohamad et al.(2006), the Young's modulus is reported to be around 13.7GPa with Poisson's ratio of 0.15 .

Figure 4.2.2.1 shows the connection between granite and mortar of the façade.

### **4.3 Modelling of the Structure**

#### **4.3.1 Linear elastic analysis**

The linear elastic analysis was used throughout the analysis. The linear elastic analysis is the procedure usually followed in structural analysis, where the material is considered to exhibit a linear elastic behaviour, both in compression and tension. In the case of masonry structures, where joints take relatively low tensile strength, cracks arise at low stress levels and, therefore, the assumption of elastic behaviour is quite doubtful. In

general, linear elastic analyses are not appropriate for ancient constructions. However, in a first stage of analysis, the hypothesis of linear elastic behaviour can be of great help. Linear analysis requires little input data, being less demanding, in terms of computer resources and engineering time used, when compared with non-linear methods. Moreover, for materials with higher tensile strength, linear analysis can provide a reasonable description of the process leading to the crack pattern.

Due to the ranging in properties of the above materials, both the granite and mortar will be classified into three cases by different elastic modulus. In all of the cases, no matter granite or mortar, the modulus will be assumed to be elastic for simplification. For case A granite, the elastic modulus will be of 53GPa, while 60GPa and 70GPa values will be considered for case B and C respectively. The density of granite will be set to be 2750 Kg/m<sup>3</sup> and with Poisson's ratio of 0.25. On the other hand, the elastic modulus of mortar was assumed to be 10GPa, 20GPa and 30GPa named case 1, case 2 and case 3 correspondingly. Although the Poisson's ratio may differ with different elastic modulus (a lower elasticity may induce a higher Poisson's ratio), a Poisson's ratio of 0.15 is fixed in all cases of mortar. The density of mortar was also taken to be 2000 Kg/m<sup>3</sup>.

#### **4.3.2 Analysis procedure**

The process of developing a detailed computer aided model of any three-dimensional structure begins with the reproduction of its geometry, followed by the creation of the solid model in a computer platform. Once the appropriate element types were selected within the finite element software (ABAQUS), the solid model was broken down into finite pieces through a systematic procedure of meshing. In this phase, the material input was also entered to the components of the model. With the application of loading and boundary conditions, the initial model was obtained.

To develop an accurate structural model, it was necessary to determine the physical dimensions of the system. Building survey measurements or available construction drawings can be used to locate reference points that define the curved geometry of a two-dimensional or even three-dimensional vaulted structure.

First, a two-dimensional plane stress analysis was carried out. In this analysis, the two-dimensional section layout of the Ruins of the St. Paul was developed (Figure 4.3.2.1) based on the AutoCAD drawing. Finite elements with four nodes are being used (CPS4R for ABAQUS), shown in Figure 4.3.2.2. The nodes of plane stress elements each have four degrees of freedom: two translational and two rotational. Alternatively, solid elements have three dimensions and hence a greater number of nodes can also be used for three dimensional analysis.

After development of the CAD representation and selection of the element types, the whole geometry was refined into individual elements according to a systematic procedure known as meshing the model. The shape and size of the elements impacts the solution. A mesh that is too coarse can produce inaccurate solutions, while a mesh that is too fine may result in problems with program limits on the number of nodes or elements or will result in excessive run times. The aspect ratio of the elements must also remain within reasonable limits: a control of an aspect ratio of less than four was carried out during the analysis. Similarly, the angles of corners can be neither too acute nor too obtuse. In this report, finite element studies in the finest of the mesh have been carried out by comparing the analysis according to the number of elements. In the following analysis, the model of the Ruins of the St. Paul would be meshed into different numbers of elements (Figure 4.3.2.3).

As mentioned in Section 2.1, there are three main types of modelling masonry approach, namely, detailed micro-modeling, simplified micro-modeling and macro modeling (Figure 4.3.2.4). In the present study, macro-modeling approach in which the structure is idealized as continua is adopted.

In this study, a two-dimensional plane stress analysis of a selected part of the structure is used to calibrate material parameters of simplified isotropic marco-model. First, a representing portion of brick pattern is selected from the Ruins of the St. Paul. (Figures 4.3.2.5 (a), 4.3.2.5 (b) and 4.3.2.5 (c)) This representing portion of brick pattern acts as the micro- modeling and is eventually homogenized to macro- modeling. This is the homogenization process (Figure 4.3.2.6), that is, to convert the combined properties of unit and mortar to a homogenized continuum. This method of analysis helps to reduce the complexity and is good enough for analysis in elastic range. However, the whole material properties will then depend on the homogenized continuum and also, information on joints or bonds are not known.

### **4.3.3 Homogenization of wall panel**

A wall panel with dimension of 1.8 m in width and 1.85 m in height was selected for homogenization as shown in Figure 4.3.2.5 (c). It was modeled as a two-dimensional plane stress wall panel with 10mm thick mortar (Figure 4.3.3.1). For determination of equivalent elastic properties of the homogenized wall panel, material properties of Case B2 are selected to perform the analysis as both the elastic modulus of granite and mortar is of average in the considered range. Granite with elastic modulus of 60GPa, Poisson's ratio of 0.25 and density of 2750 Kg/m<sup>3</sup> were considered; whereas for mortar, values of 20GPa, 0.15 and 2000 Kg/m<sup>3</sup> were employed. The wall panel was then meshed into 33300 elements with elements having a global size of 10 mm (Figure 4.3.3.2). The

loading condition will be at uniform pressure of 100MPa exerted at the top of the wall panel with its self weight and with boundary conditions pinned at the bottom. (Figure 4.3.3.3) The deformation of the wall was then measured as shown in Figure 4.3.2.4 and thus, knowing the lateral and longitudinal strain of the assembly.

The lateral strain and longitudinal strain will be calculated and thus, the elastic modulus and Poisson's ratio of the assembly. Here are the equations used.

$$\epsilon_{long} = \frac{\delta}{L} \quad (\text{Eq. 1})$$

$$\epsilon_{lat} = \frac{\delta'}{L} \quad (\text{Eq. 2})$$

$$\nu = -\frac{\epsilon_{lat}}{\epsilon_{long}} \quad (\text{Eq. 3})$$

$$E = \frac{\sigma}{\epsilon} \quad (\text{Eq. 4})$$

Where  $\delta$  = displacement along longitudinal direction;  $\delta'$  = displacement long lateral direction; L = original length of the structure and  $\sigma$  = normal stress

Before carrying out the analysis of the program, verification of the model is also essential. This was done by assigning the whole model with only one material property, for example, granite. The verification was done by backing calculation of the modulus of elasticity of the material and comparison with the input value. The modulus of elasticity was 60GPa with Poisson's ratio of 0.25. The loading condition will be a uniform pressure of 100MPa exerted at the top of the wall panel and with boundary conditions pinned at the bottom. The average deformation was calculated and shown in Table 4.3.2.1. The main purpose was to back calculate the elastic modulus to verify the mesh and determine the accuracy. The elastic modulus, as a result, was computed to be 60.617GPa (using Eqs 1 to 4). There was a difference of 1.03% in value to that of the input, which can safely be considered as satisfactory.

Another important verification was the application of the self weight to the model. The same conditions were applied as mentioned above. Except that for the loading condition, it will be of self weight of the panel only instead of the 100MPa pressure. The stress, in the vertical direction, ( $S_{22}$ ) of the lowest element was calculated first by Eq (5).

$$\sigma_{22} = \rho g H \quad (\text{Eq. 5})$$

Where  $\rho$  = density,  $g$  = gravity,  $H$  = height

$$\sigma_{22} = 2750(9.81)(1.85) = 49908.38 \text{ Pa}$$

After that, the value of the vertical stress a few elements at the lowest level was being computed. The values are shown in Table 4.3.3.2 with an average of 48367.1 Pa. This value differs in 3.09% to that of the theoretical one, which is again a fairly good accuracy.

Finally, the analysis can be started after the above verification. And most importantly, the properties of the homogenized continuum were found out (by Eqs1-4) to be a material of having elastic modulus of 57.98GPa and Poisson's ratio of 0.2448 (Figures 4.3.3.3 and 4.3.3.4). These properties were very close to that of the granite and it is understandable since granite was the main portion of the wall panel.

These properties of the homogenized continuum were then used as the material properties of the façade. Since the façade was mainly constructed with granite, the density of granite, 2750 Kg/m<sup>3</sup> was achieved. The weight of the decorations and statues at the front of the façade was neglected. The façade with its self weight was simulated with boundary conditions pinned at the bottom. The purpose of the loading was to simulate when the façade is subjected to its self weight and investigate the effect when dealing to its own self weight. Thus, the stress strain distribution and the deformation can be known. However, the pattern of the arrangement of the unit and cracks did not take into account, as well as the stress between the unit and the mortar. The detailed analysis will be discussed in the following section.

#### **4.4. Analysis and Parametric Study of the wall panel.**

##### **4.4.1 General**

As mention in the previous section, the selected portion (Figure 4.3.4.5 (c)) was being modeled as a two-dimensional plane stress wall panel with 10mm thick mortar and the dimensions were 1.8m in width and 1.85m in height (Figure 4.3.2.1). And both the granite mortar will be classified in three cases by different elastic modulus because of the ranging in properties. For case A granite, the elastic modulus will be 53GPa, while 60GPa and 70GPa for case B and C respectively. The density of granite is set to be 2750 Kg/m<sup>3</sup> and with a Poisson's ratio of 0.25. On the other hand, the elastic modulus of mortar is assumed to be 10GPa, 20GPa and 30GPa with case 1, case 2 and case 3 correspondingly. Poisson's ratio of 0.15 is fixed in all cases of mortar. A summary of the material properties of each case was shown in Table 4.4.1.1. And the loading condition will be a uniform pressure of 100MPa exerted at the top of the wall panel with its self weight and with boundary conditions pinned at the bottom.

Case B2 with the finest mesh model (number of elements = 33300) will be discussed since case B2 is of average Young's modulus for both materials. Moreover, finest mesh is more desirable for analysis. The analysis results are shown in Figure 4.4.1.1 to 4.4.1.8. In discussing the horizontal stress of the wall panel, shown in Figure 4.4.1.1. Excluding the compression at the bottom due to the constraint, the mortar in the horizontal will exert great compression strength. Tensile stresses will be exerted at the granite element around the junction.

It can be obviously seen that the minimum compression stress occurs at the location of the mortar oriented along the direction of the applied pressure. This is probably because of the difference in the material properties. As the elastic modulus of the granite is

higher, it can be clear that the granite part will have a higher compression stress in order to maintain the compatibility condition. And also, due to the difference in material properties, the strain of the mortar will be higher. However, the elongation of both materials should be the same; thus, internal stress is induced to the retaining of the compatibility. Figure 4.4.1.8 shows the maximum in plane principal stress for the panel.

#### **4.4.2 Mesh study of the wall panel**

In developing the mesh of the wall panel, several meshes with a difference in total number of elements have been developed. A coarse mesh, with 2256 elements, was first generated with approximate global element size of 0.04m and the aspect ratio was control within 1:4. (Figure 4.4.2.1) Analysis was then carried out using this mesh and the maximum principal stress of some critical points will be discussed. (Figure 4.4.2.2) Region A is mainly the granite element where the maximum in plane principal stress occurs. Region B is also the granite element where the minimum in plane principal stress takes place. For mortar element, region C will be discussed where this was the point of junction of the mortar.

After defining these critical locations, other meshes were further developed. Finer meshes, with 8742 and 15004 elements, were then generated with approximate global element size of 0.02m and 0.015m respectively. (Figures 4.4.2.3 and 4.4.2.4) And finally, a finest mesh (Figure 4.4.2.5) with 33300 was developed and the element size was 0.01m by 0.01m, which was exactly the thickness of the mortar. This mesh, despite of its fineness, has of a comparatively high number of elements. Tables 4.4.2.1 and 4.4.2.2 show the maximum in plane principal stress at different locations of different meshes. The ratio of the stress values between different meshes with that of the finest mesh was computed. The purpose of computing these ratios was to normalize the stress value for

Advanced Master in Structural Analysis of Monuments and Historical Constructions

the ease of comparison. Figure 4.4.2.6 shows the convergence of the normalized stress value. The result showed that the mesh with 8742 elements was around 90 percent as good as that of the finest one. While the mesh with 15004 elements with difference in value of less than 5 percent, however the total number of elements was less than half of the finest one only. Therefore, it can be concluded that the mesh with 15004 elements was already far enough for analysis as it converges to the solution, and the total number of elements can be reduced by half.

#### **4.4.3 Effects of elastic modulus**

Different cases are then being analysed with different combinations of granite and mortar. The stress, strain and displacement contour patterns in a similar way for all cases but differ in values. Tables 4.4.3.1 and 4.4.3.2 are summaries of the principal in plane stress of the different combination of mortar and granite, that is, cases A1, A2, A3, B1, B2, B3, C1, C2 and C3. Figures 4.4.3.1 to 4.4.3.4 show the variations of the stress value with variations of the elastic modulus of mortar and granite. The trend of these curves can be observed. The results showed that variation would be quite linear for this particular wall panel.

### **4.5 Analysis of the two dimensional plane of the façade**

#### **4.5.1 General**

The model of the Ruin of the St. Paul followed similar procedures as the wall panel. And the façade was modeled to be subject to its own self weight pinned at the bottom. CPS4R elements were used and the finest model was meshed into 122384 elements with global size of elements of 0.05m and the aspect ratio was control within 1:4. (Figure 4.5.3) The result contours, such as the stress, strain and deformation, were shown in Figures 4.5.1.1 to 4.5.1.8.

#### 4.5.2 Mesh study of the façade

In developing the mesh of the façade, several meshes were again being developed similar to that of the developing of the wall panel. A coarse mesh, with 7659 elements was first generated. This mesh was generated automatically with approximate global element size of 0.2m. (Figure 4.5.2.1) Figure 4.5.2.2 shows the four locations where the stress distributions were critical and will be set as interest regions for the mesh study. Region A is mainly at the arch of the door on the right side while region C was the part at the window in the middle where at both regions, tension occurs. Regions B and C were the compression areas beside the arches.

After defining these critical points, other meshes were further developed. A finer mesh, with 30991 elements, was then generated with approximate global element size of 0.1m. (Figure 4.5.2.3) The finest mesh (Figure 4.5.2.4), which was mentioned previously, was used as a base. This mesh contained a high number of elements. Tables 4.5.2.1 and 4.5.2.2 show the maximum in plane principal stress at different locations of different meshes. The ratio of the stress values between different meshes with that of the finest mesh was computed. The normalized stress value was used as comparison based on the stress value obtained from the finest mesh,  $S_{122384}$ . Figure 4.5.2.5 shows the convergence of the normalized stress value. The result showed that the stress values obtained from the mesh with 7659 elements had quite a difference compare to that of the finest one. Especially the stress at region D, the difference was quite obvious. The mesh with 30991 elements with difference in value of less than 10 percent, however the total number of elements was only of around one quarter to that of the finest one. It can also be concluded that the mesh with 30991 elements was already far enough for analysis as it converges to the solution. And the total number of elements can be greatly reduced.

After this approach, further meshes were being developed in order to reduce the total number of elements while giving precise result. As the critical zones were mainly located around the windows and the doors, these locations should be even better defined. Figure 4.5.2.6 shows the finite element mesh developed by adjusting the number of nodes at the windows and at the arch of the doors. This mesh was generated by seeding the size of the exterior edge with 0.5m while 0.05m for the interior windows and for the arch at the doors. This mesh showed better precision compare to that of the coarse one (the mesh with 7659 elements) probably because the defined critical regions A, B, C contains more elements. However, this was not as good as the previous (the finest mesh with 122384 elements) as many of the elements generated was of an aspect ratio larger than four. And many of these were in the defined critical regions A, B, C. This greatly reduced the accuracy and thus another mesh was developed. Figure 4.5.2.7 shows the locations where were seeded with 0.05m while the exterior edge was seeded with 0.5m. Figure 4.5.2.8 shows the meshing where the defined critical regions A, B, C consist of finer meshes and a coarser mesh at other locations. Tables 4.5.2.3 and 4.5.2.4 show the maximum in plane principal stress at different locations of different meshes as well as the normalized stress based on the finest mesh.

### **4.5.3 Discussion of finite element results of the facade**

In considering the stress in the horizontal direction, compression occurs at the bottom and the two sides of the arch at the door of the façade. (Figure 4.5.1.1) The compression at the bottom is caused by the constraint at the ground due to the geometry of the façade, maximum compression occurs at the two sides of the arch. At the top arch of every window and door, tensile stress will be of maximum. At the mid way of the structure, in between the door and the window, the section is consisting of regions of tension and compression as shown in Figure 4.5.1.1.

For the vertical stress contour, the compression exert to the whole facade is easily understood as its self weight acts downward to the bottom. The tension region appears mainly at the area between the door and the window. Figure 4.5.1.8 shows the maximum in plane principal stress for the façade. The maximum principle stress values for tensile stress were around +0.21MPa while -0.22MPa for compressive stress. The values for both tension and compression are low, corresponding to linear elastic analysis of structure subject to self weight only. However, possible checking may be required for critical points where high tensile stresses are located.

Table 4.3.3.1 Table of summary of the values obtained for the verification of the applied loading to the model

nodes ID	U: U2 (mm)
1907	-3.05279
1906	-3.05258
1905	-3.05237
1904	-3.05217
1903	-3.05197
1902	-3.05178
1901	-3.05160
1900	-3.051420
1899	-3.05125
1898	-3.051090
Average	-3.051902

Table 4.3.3.2 Table of summary of the values obtained for the verification of the self weight applied to the model.

element ID	S: S22(Pa)
29124	-48359.2
29125	-48366.3
29126	-48373
29127	-48379.4
29128	-48385.5
29129	-48391.3
29130	-48396.7
29131	-48401.9
29132	-48406.6
29217	-48210.7
Average	-48367.1

Table 4.4.1.1 summary of material properties in all cases

case	elastic modulus (GPa)		Poisson's ratio		Density (kg/m <sup>3</sup> )	
	unit	mortar	unit	mortar	unit	mortar
A1	53	10	0.25	0.15	2750	2000
A2	53	20	0.25	0.15	2750	2000
A3	53	30	0.25	0.15	2750	2000
B1	60	10	0.25	0.15	2750	2000
B2	60	20	0.25	0.15	2750	2000
B3	60	30	0.25	0.15	2750	2000
C1	70	10	0.25	0.15	2750	2000
C2	70	20	0.25	0.15	2750	2000
C3	70	30	0.25	0.15	2750	2000

Table 4.4.2.1 Maximum in plane principal stress at different locations of different meshes

No. of elements		A	B	C
		Stress (10 <sup>6</sup> )	Stress (10 <sup>6</sup> )	Stress (10 <sup>6</sup> )
2,256	Value	2.73	-22.74	-9.20
	At Element	1927	2,016	165
8,742	Value	3.87	-23.31	-11.32
	At Element	7531	7,716	326
15,004	Value	4.19	-23.42	-11.95
	At Element	12891	13,131	426
33,300	Value	4.18	-23.50	-12.31
	At Element	28786	29,147	636

Table 4.4.2.2 Normalized plane principal stress at different locations of different meshes

	A	B	C
No. of elements	Stress ( $10^6$ )	Stress ( $10^6$ )	Stress ( $10^6$ )
2,256	0.65	0.97	0.75
8,742	0.92	0.99	0.92
15,004	1.00	1.00	0.97
33,300	1.00	1.00	1.00

Table 4.4.3.1 Principal stress (MPa) at location A for different cases.

Location A		Elastic modulus of Granite (GPa)		
		A (53)	B (60)	C (70)
Elastic modulus of mortar (GPa)	10	6.14	6.57	7.11
	20	3.77	4.18	4.70
	30	2.53	2.89	3.36

Table 4.4.3.2 Principal stress (MPa) at location C for different cases.

Location C		Elastic modulus of Granite (GPa)		
		A (53)	B (60)	C (70)
Elastic modulus of mortar (GPa)	10	-15.78	-16.36	-16.99
	20	-11.35	-12.31	-13.40
	30	-7.49	-8.80	-10.26

Table 4.5.2.1 Maximum in plane principal stress at different locations of different meshes

		A	B	C	D
		S(10 3)	S(10 3)	S(10 3)	S(10 3)
7,659	Value	168.47	-136.25	179.86	-102.51
	At Element	1870	1,985	2819	6,159
30,991	Value	195.80	-143.35	198.60	-146.48
	At Element	7998	10,887	11831	25,422
122,384	Value	208.61	-146.27	212.04	-147.84
	At Element	31265	42,700	62628	9,993

Table 4.5.2.2 Normalized plane principal stress at different locations of different meshes

		A	B	C	D
		S(10 3)	S(10 3)	S(10 3)	S(10 3)
7,659	Value	168.47	-136.25	179.86	-102.51
30,991	Value	195.80	-143.35	198.60	-146.48
122,384	Value	208.61	-146.27	212.04	-147.84

Table 4.5.2.3 Maximum in plane principal stress at different locations of different meshes

		A	B	C	D
		S(10 3)	S(10 3)	S(10 3)	S(10 3)
13,617	Value	193.68	-156.74	165.76	-130.33
	At Element	1446	3,713	7304	11,776
24,565	Value	208.79	-145.88	203.53	-136.76
	At Element	22565	18,210	17460	24,195
122,384	Value	208.61	-146.27	212.04	-147.84
	At Element	31265	42,700	62628	99,993

Table 4.5.2.4 Normalized plane principal stress at different locations of different meshes

		A	B	C	D
		S(10 3)	S(10 3)	S(10 3)	S(10 3)
13,617	Value	0.93	1.07	0.78	0.88
24,565	Value	1.00	1.00	0.96	0.93
122,384	Value	1.00	1.00	1.00	1.00

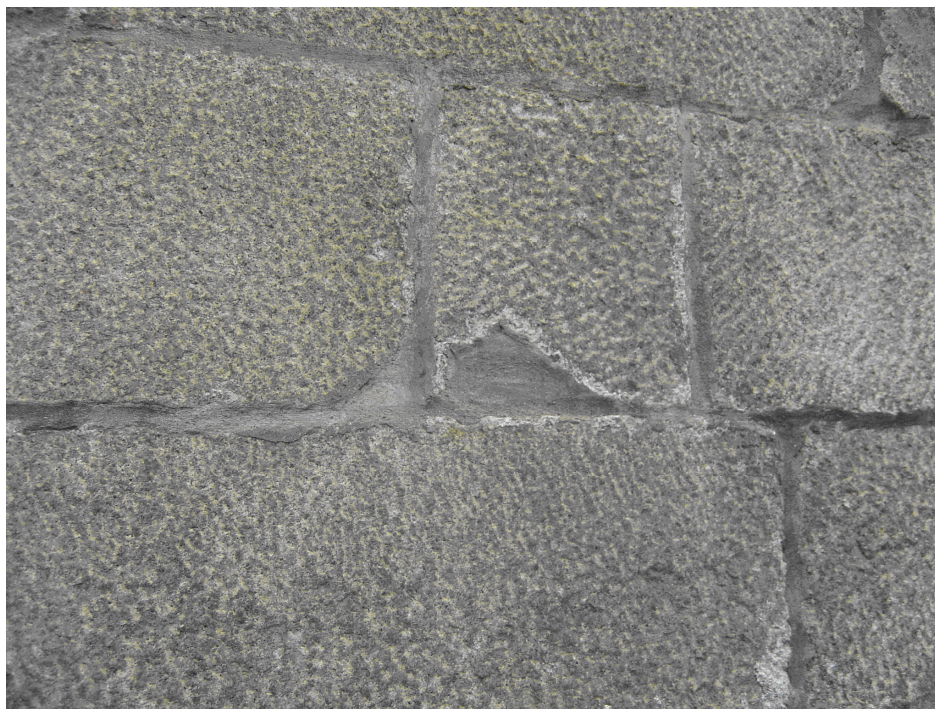


Figure 4.2.2.1 Connection between granite and mortar of the ruins of the St. Paul

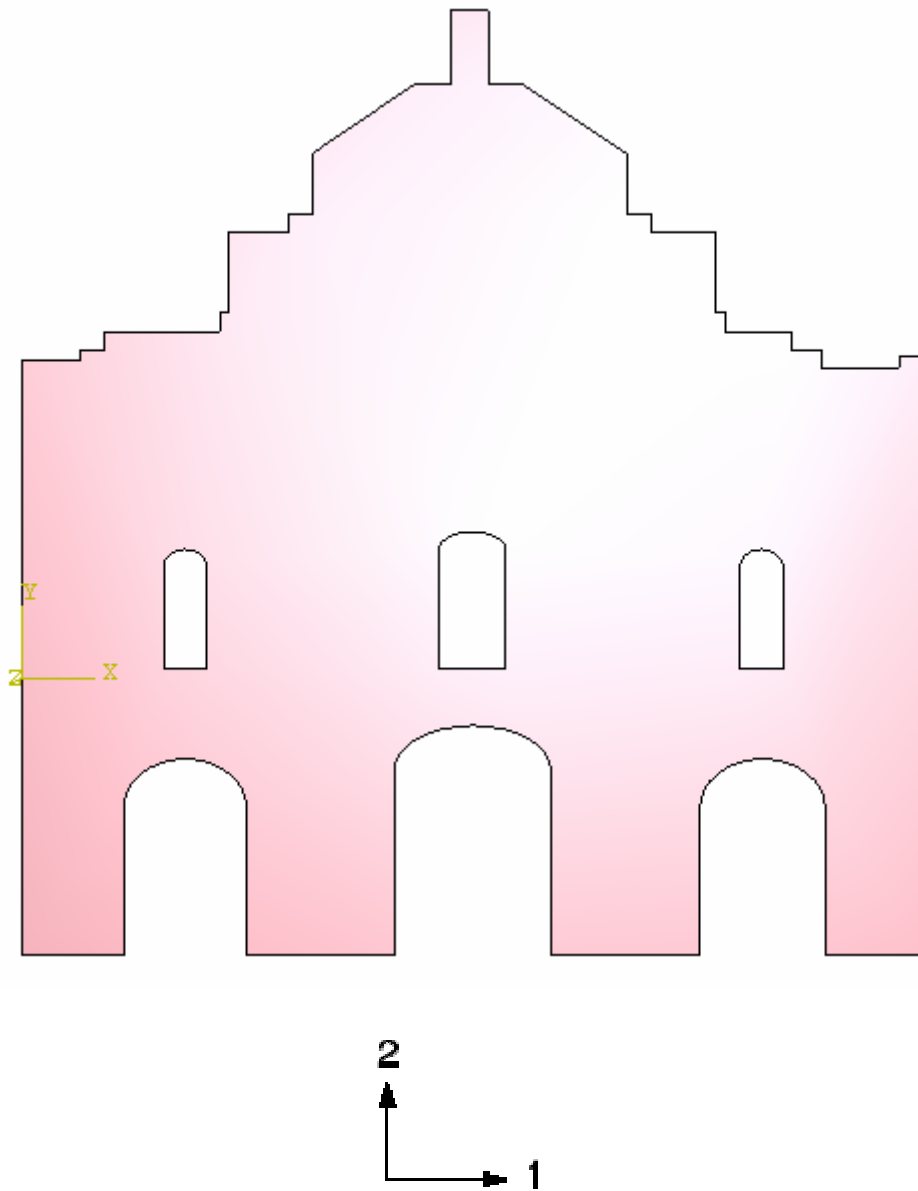


Figure 4.3.2.1 2D plane of the Ruins of St. Paul

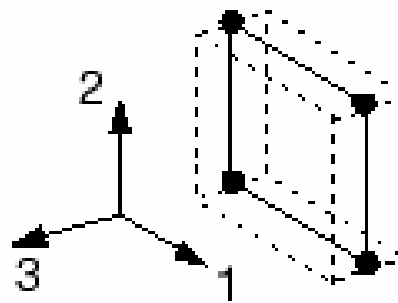


Figure 4.3.2.2 Plane stress element

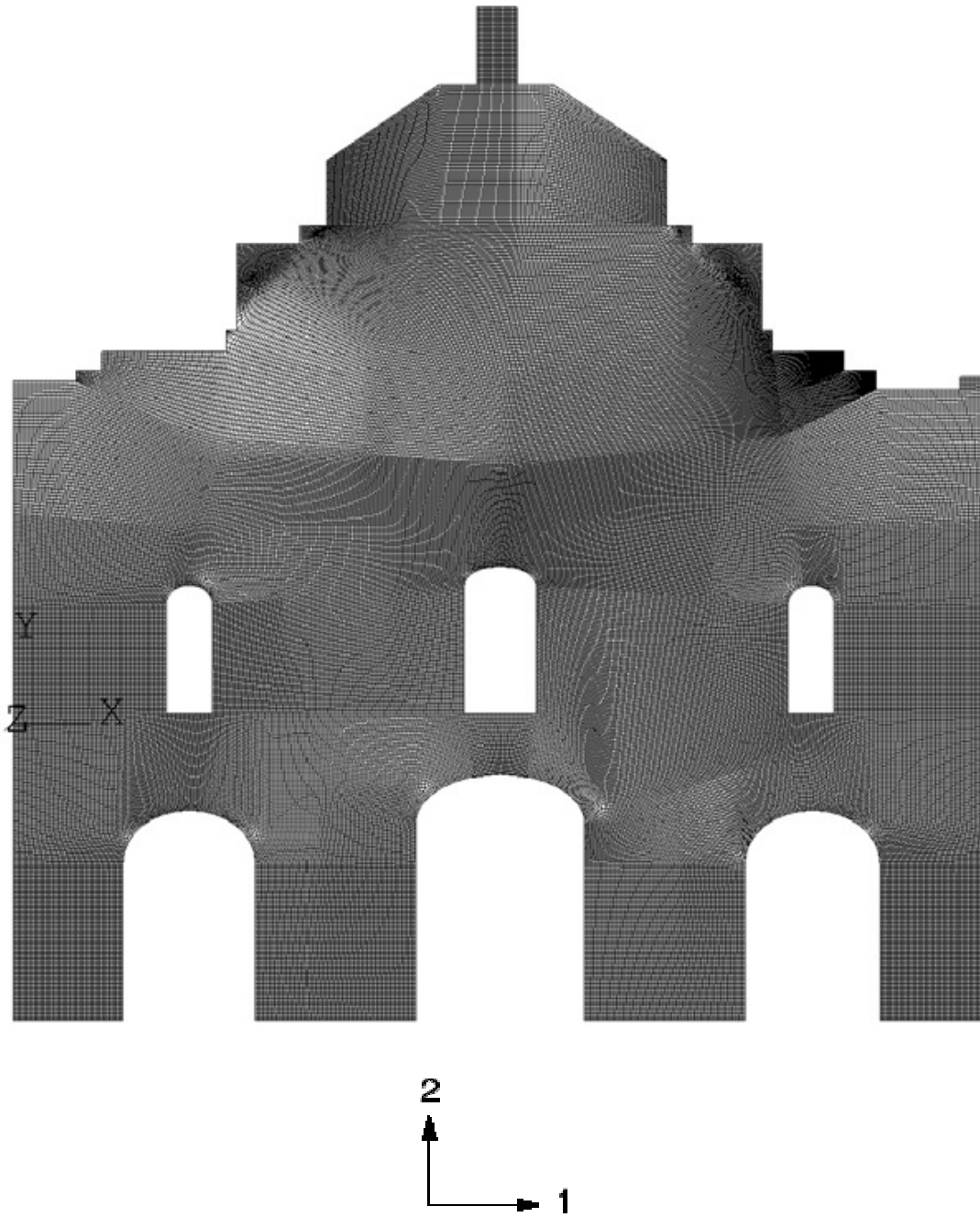


Figure 4.3.2.3 FEM mesh of the Ruins of the St. Paul (no. of elements = 122384)

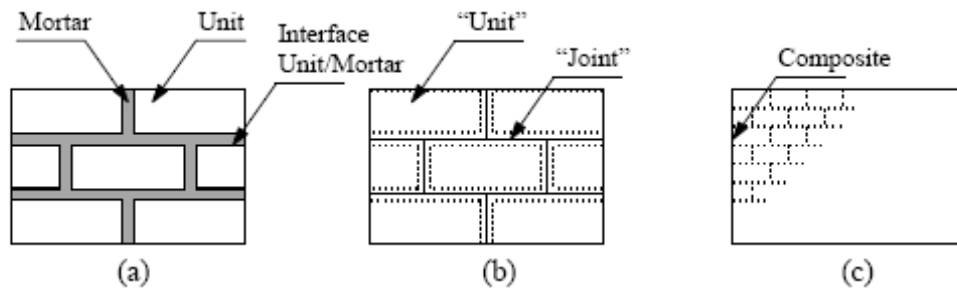
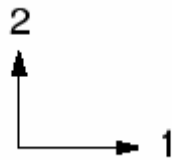
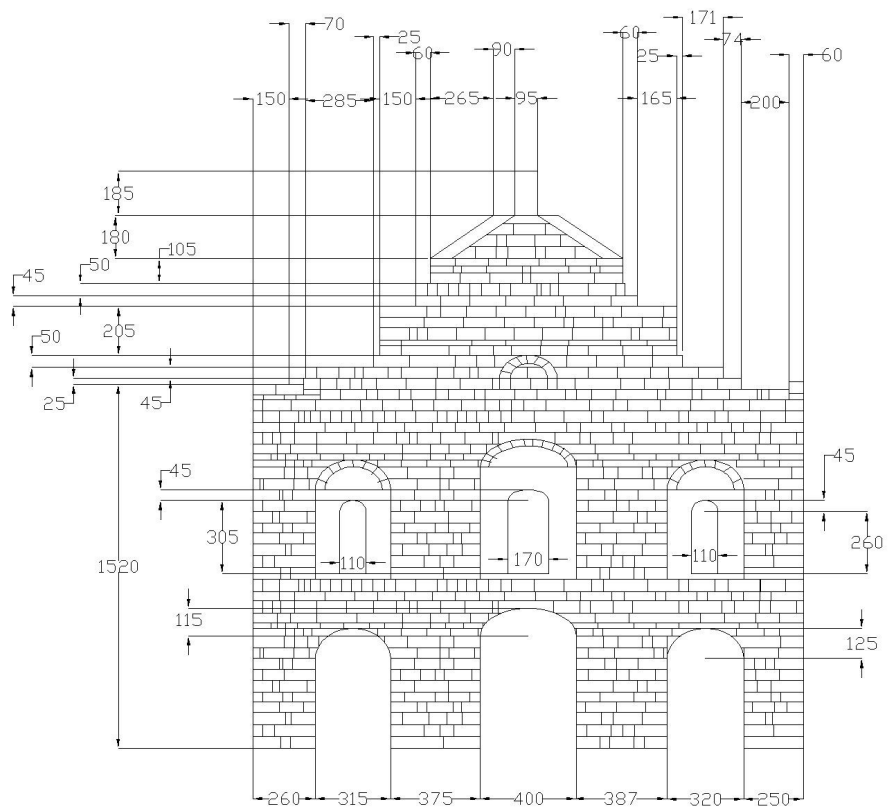


Figure 4.3.2.4 Modeling strategies for masonry structures: (a) detailed micro-modeling; (b) simplified micro-modeling; (c) macro-modeling (Lourenço (1998)).

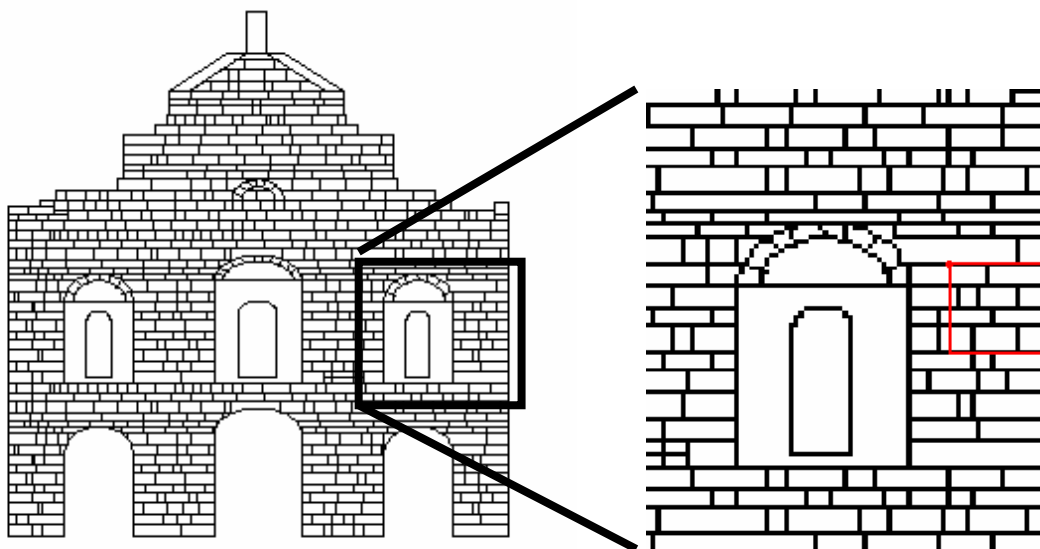


(a) Rear view of the Ruins of the St. Paul (Figure 4.3.2.5)



(b) Rear view of the ruins of the St. Paul drawn using Auto Cad (with dimensions)

(Figure 4.3.2.5)



(c) Pattern that are used to do the analysis

Figure 4.3.2.5 Selection of the representative portion

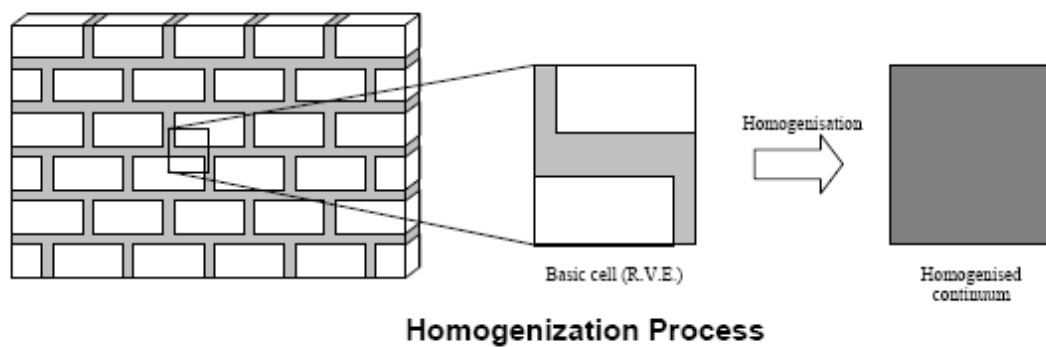


Figure 4.3.2.6 Homogenization process (Lourenço (1996))

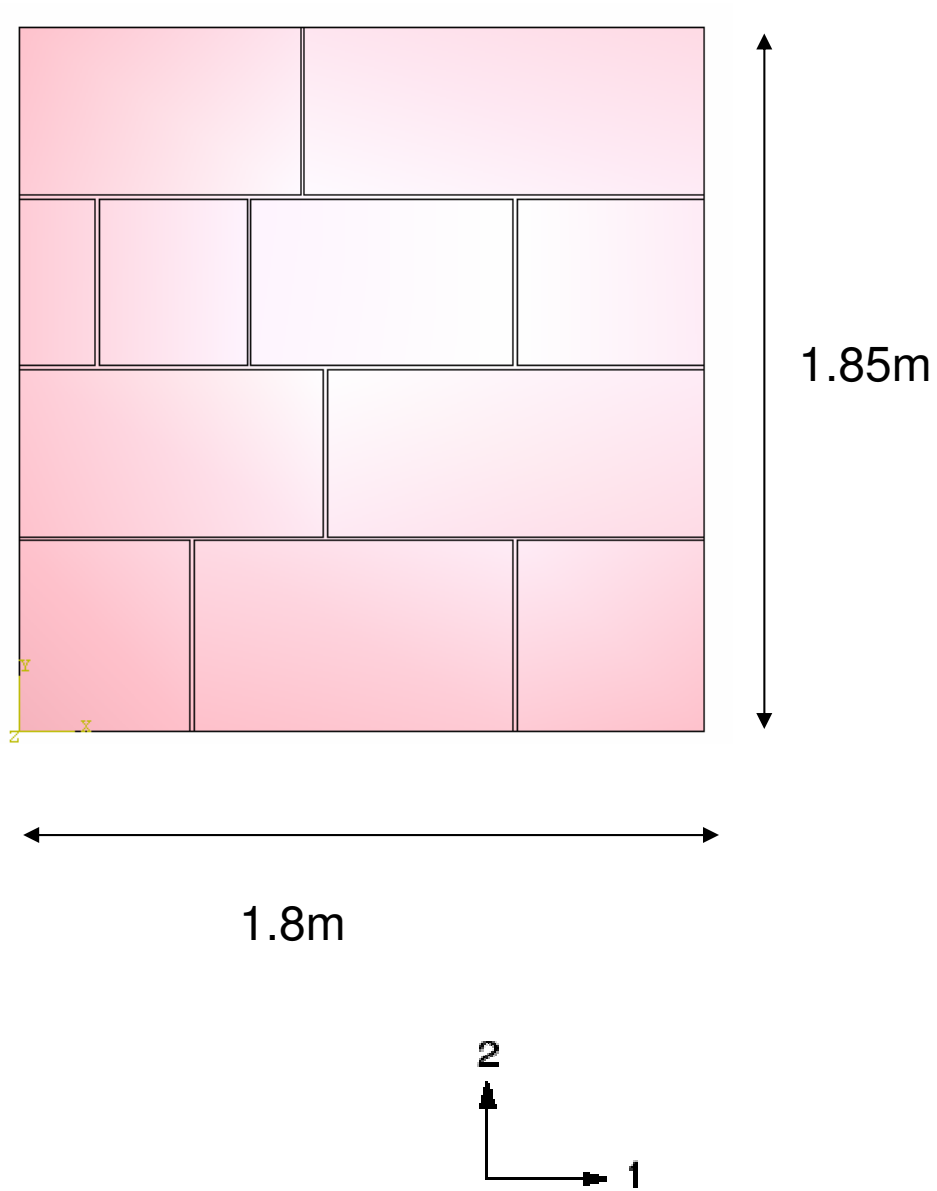


Figure 4.3.2.1 2D plane of the selected portion

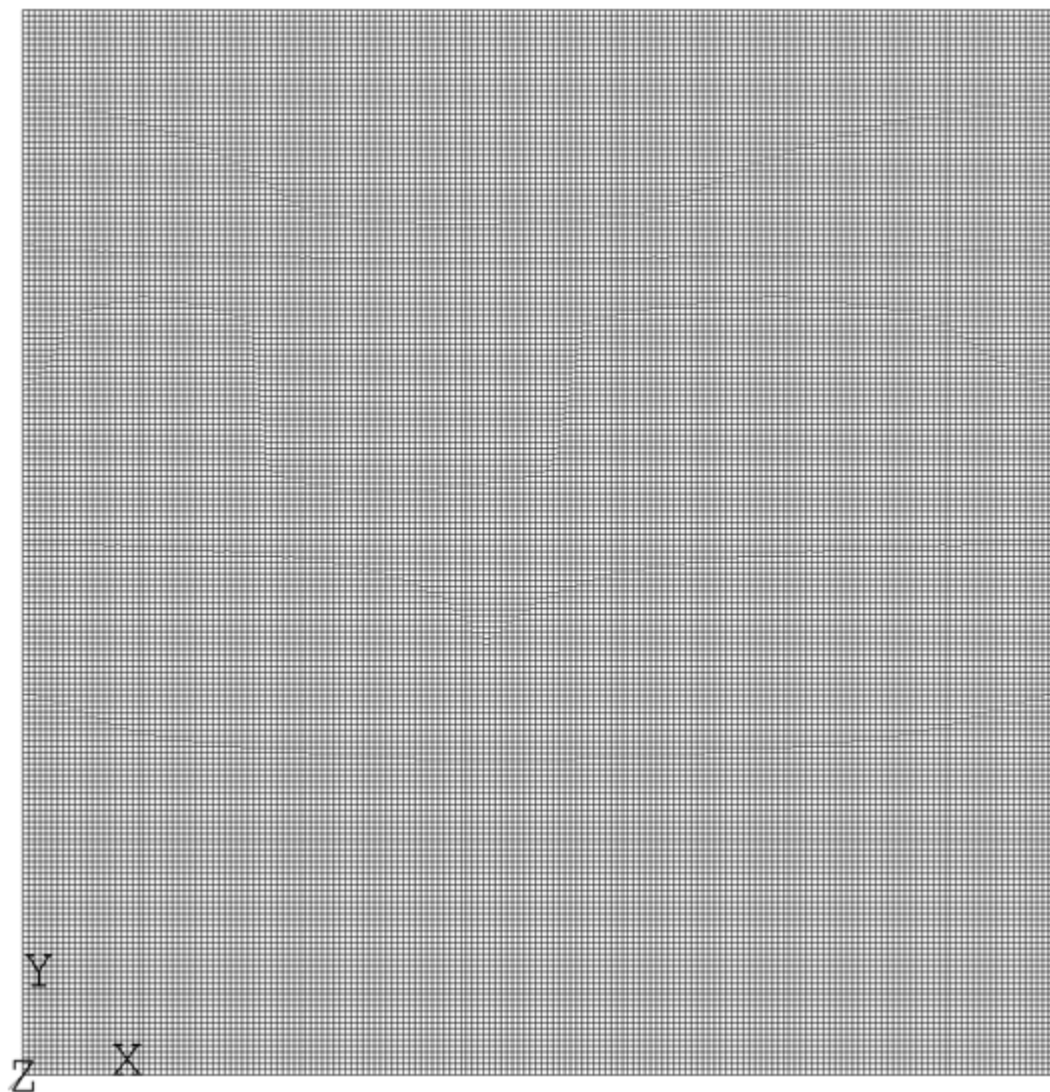


Figure 4.3.2.2 FEM mesh of selected portion (no. of elements = 33300) size of elements =10mm x 10mm

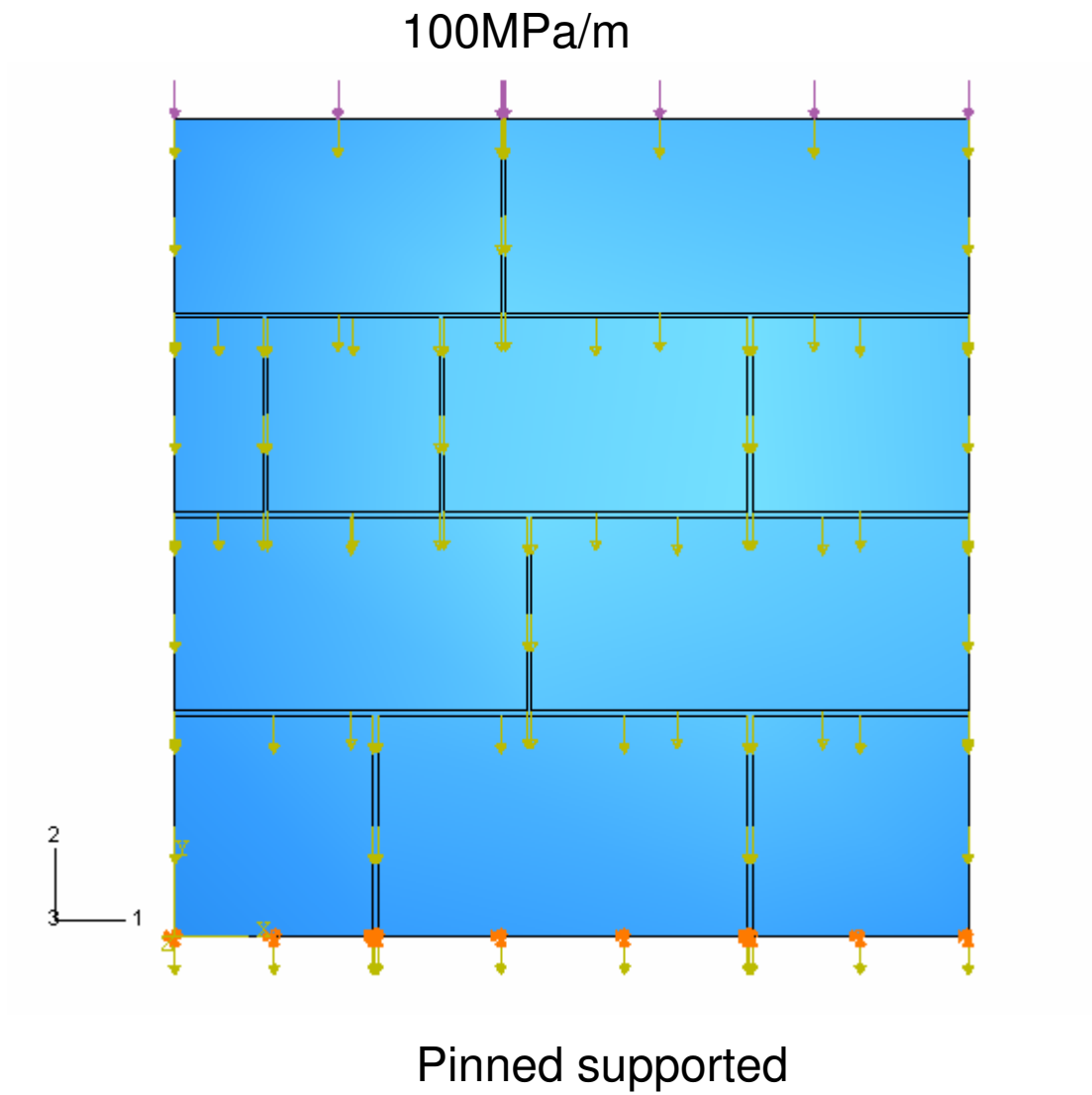


Figure 4.3.2.3 Load conditions and boundary conditions of the wall panel

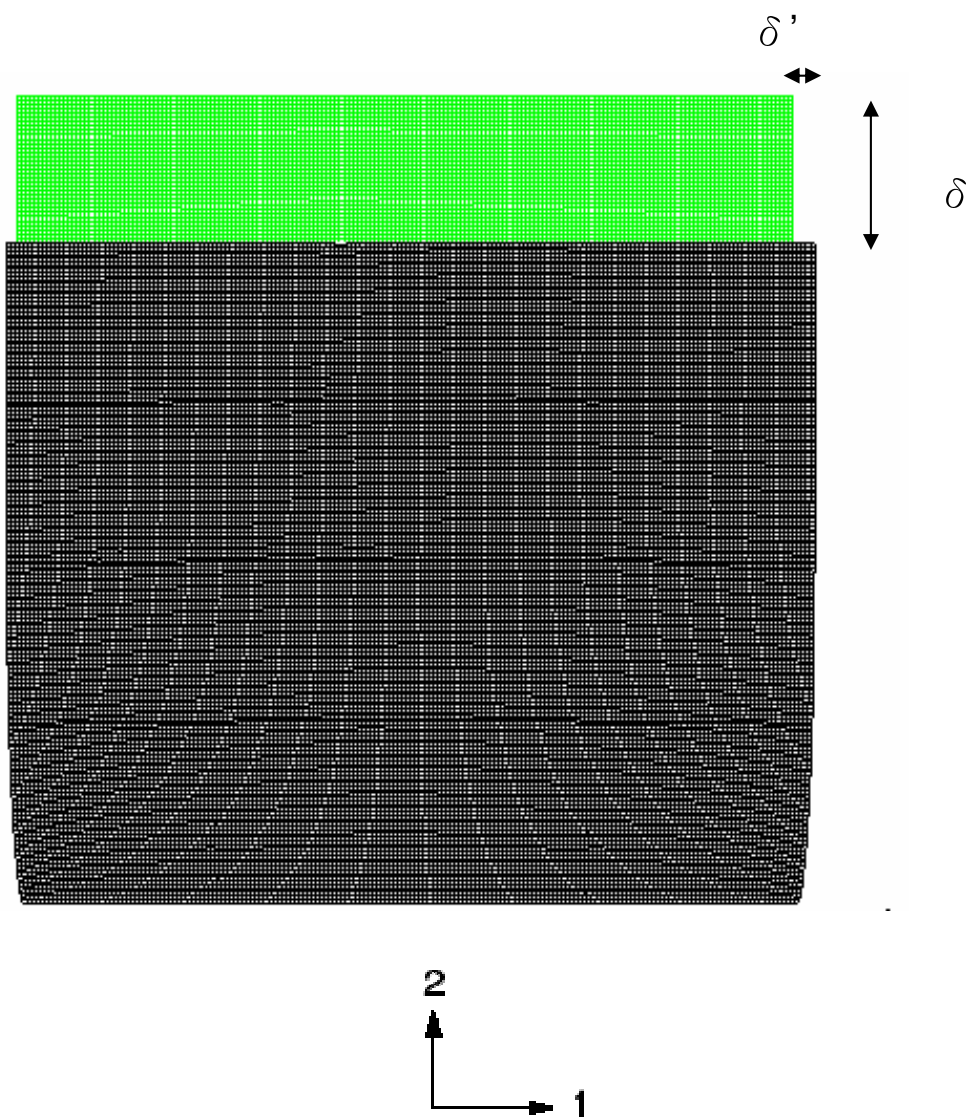


Figure 4.3.2.4 Deformation of the wall panel

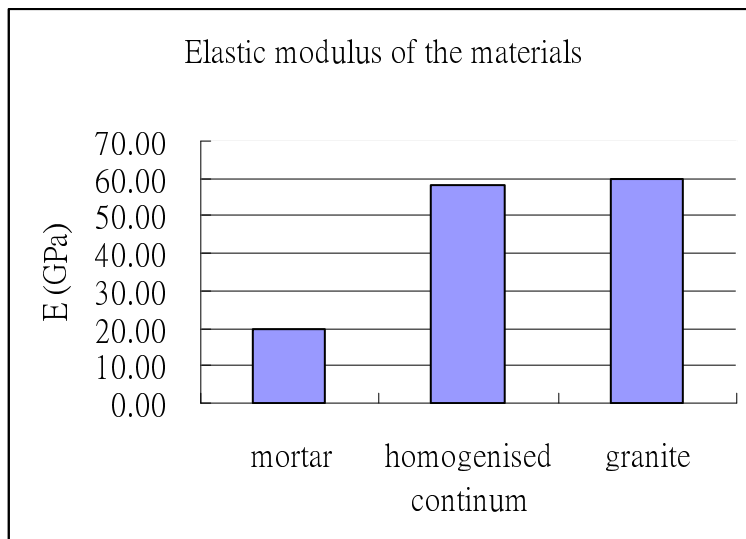


Figure 4.3.2.3 Elastic modulus of the materials

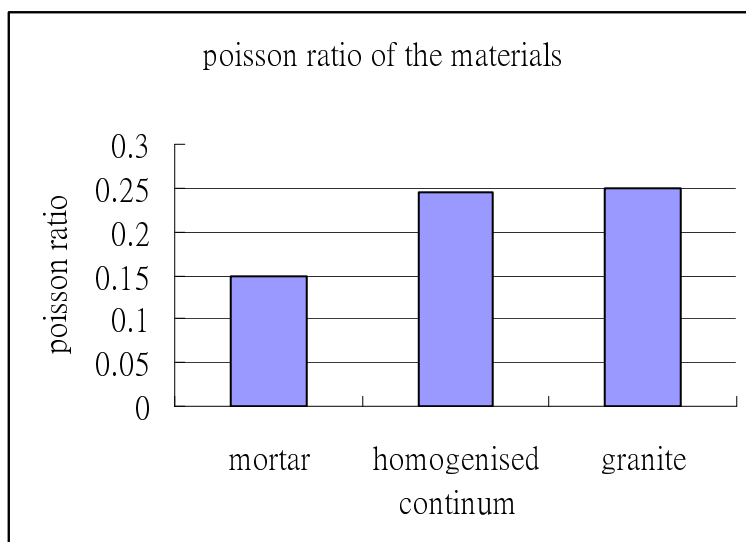


Figure 4.3.2.4 Poisson ratio of the materials

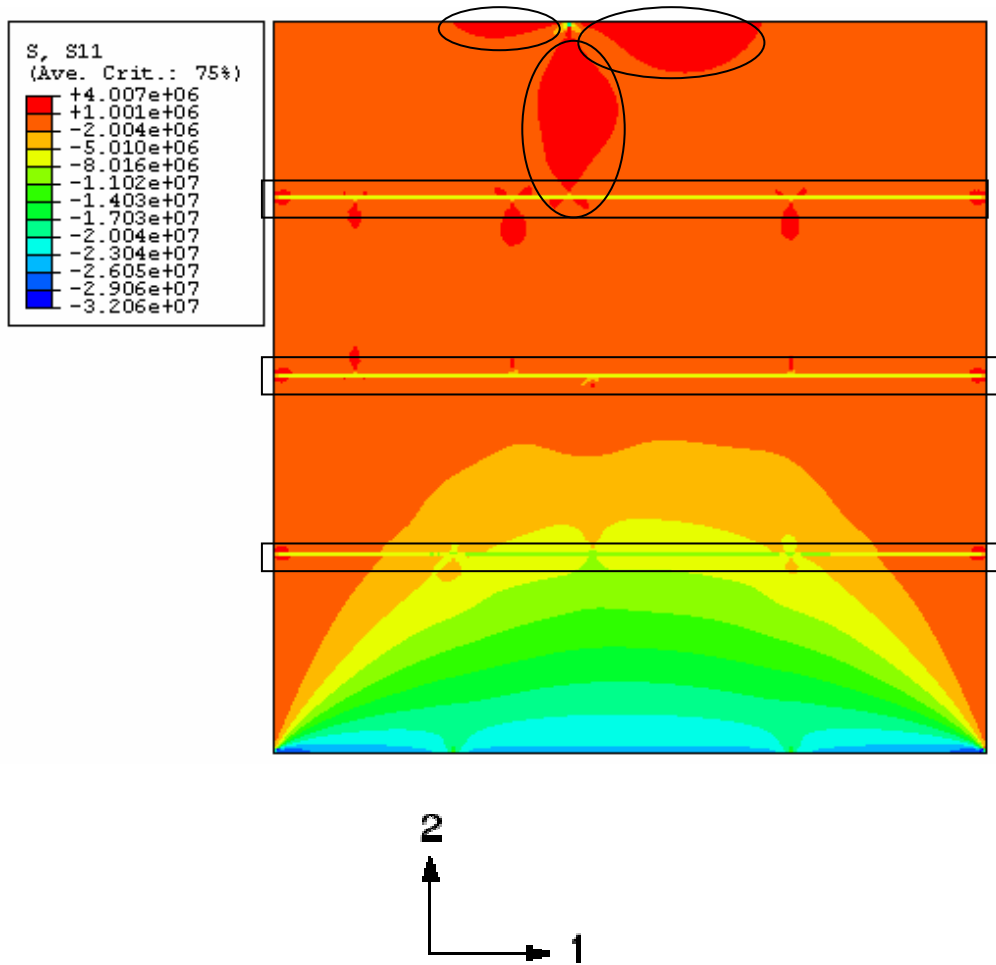


Figure 4.4.1.1 Stress 11 for case B2 panel

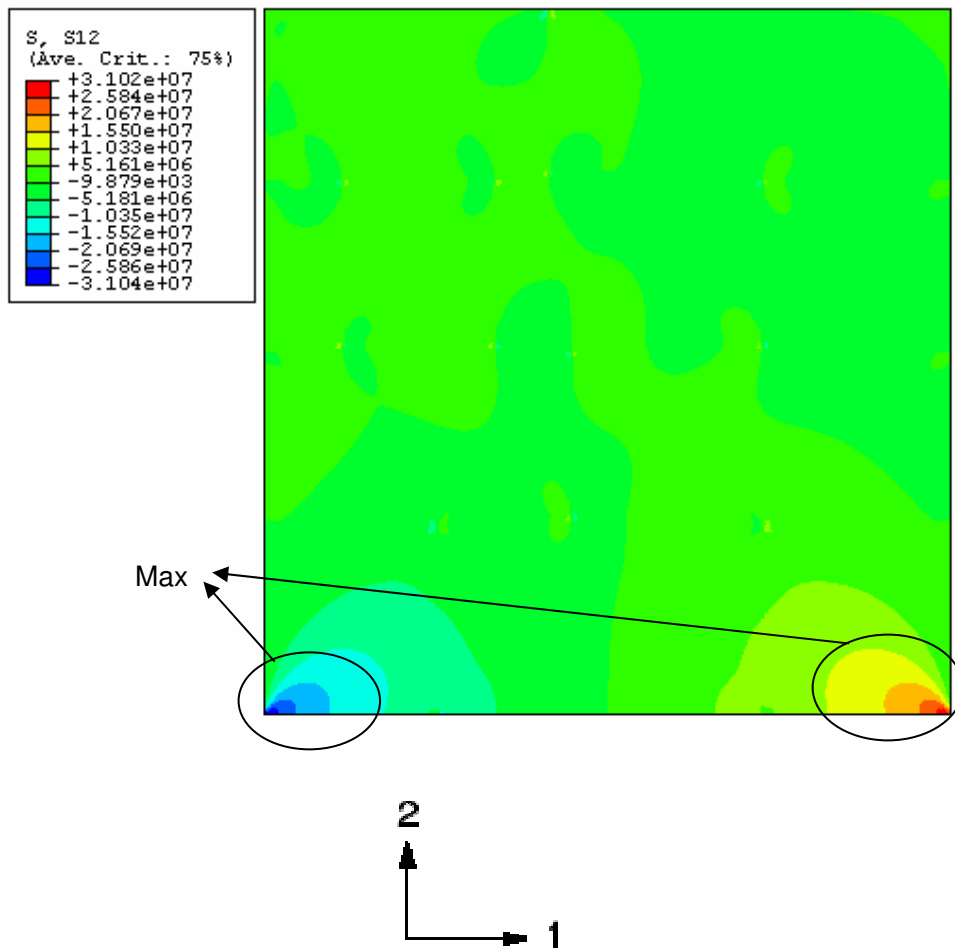


Figure 4.4.1.2 Stress12 for case B2 panel

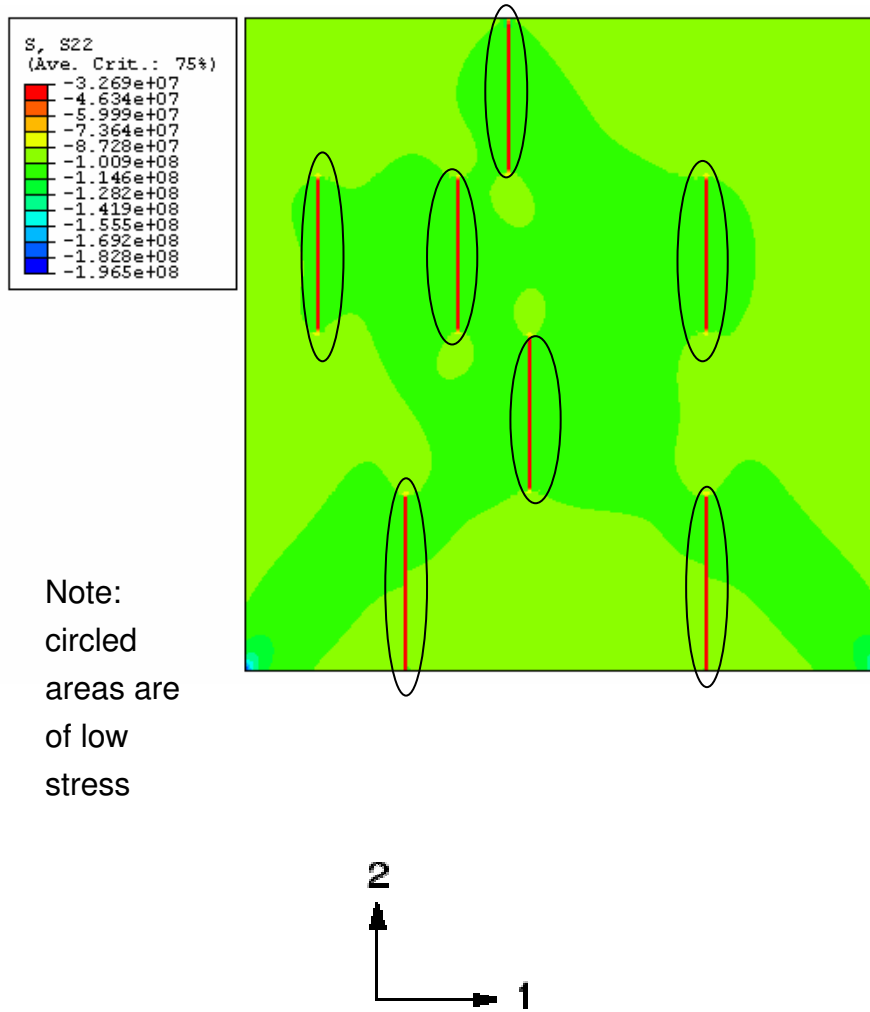


Figure 4.4.1.3 Stress 22 for case B2 panel

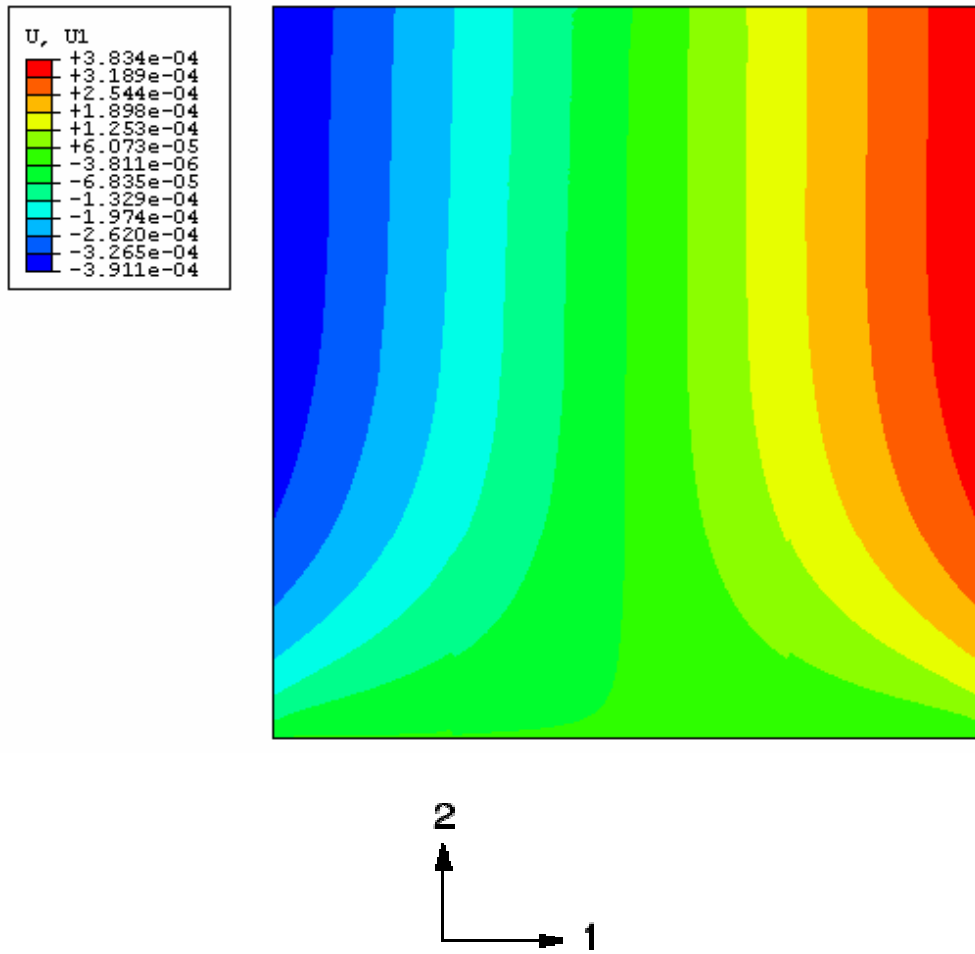


Figure 4.4.1.4 Displacement in 1-dir for case B2 panel

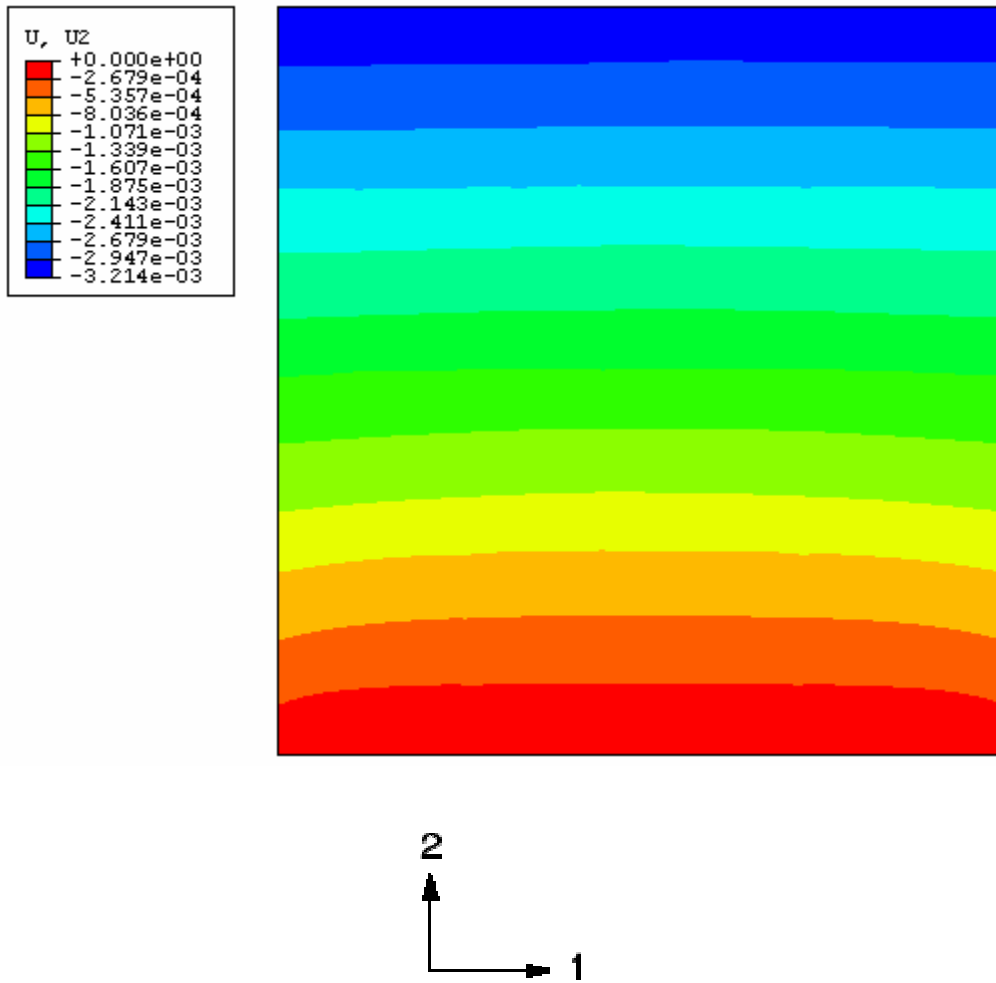


Figure 4.4.1.5 Displacement in 2-dir for case B2 panel

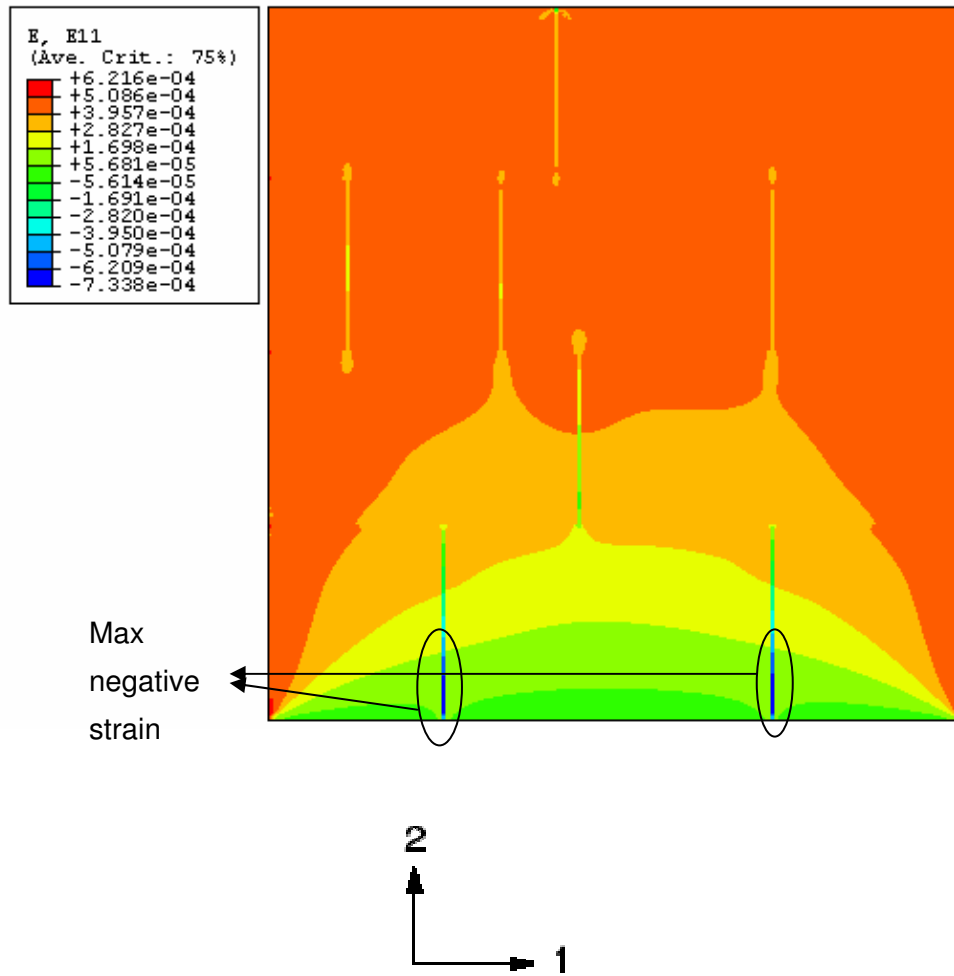


Figure 4.4.1.6 Strain components in 1-1 dir for case B2 panel

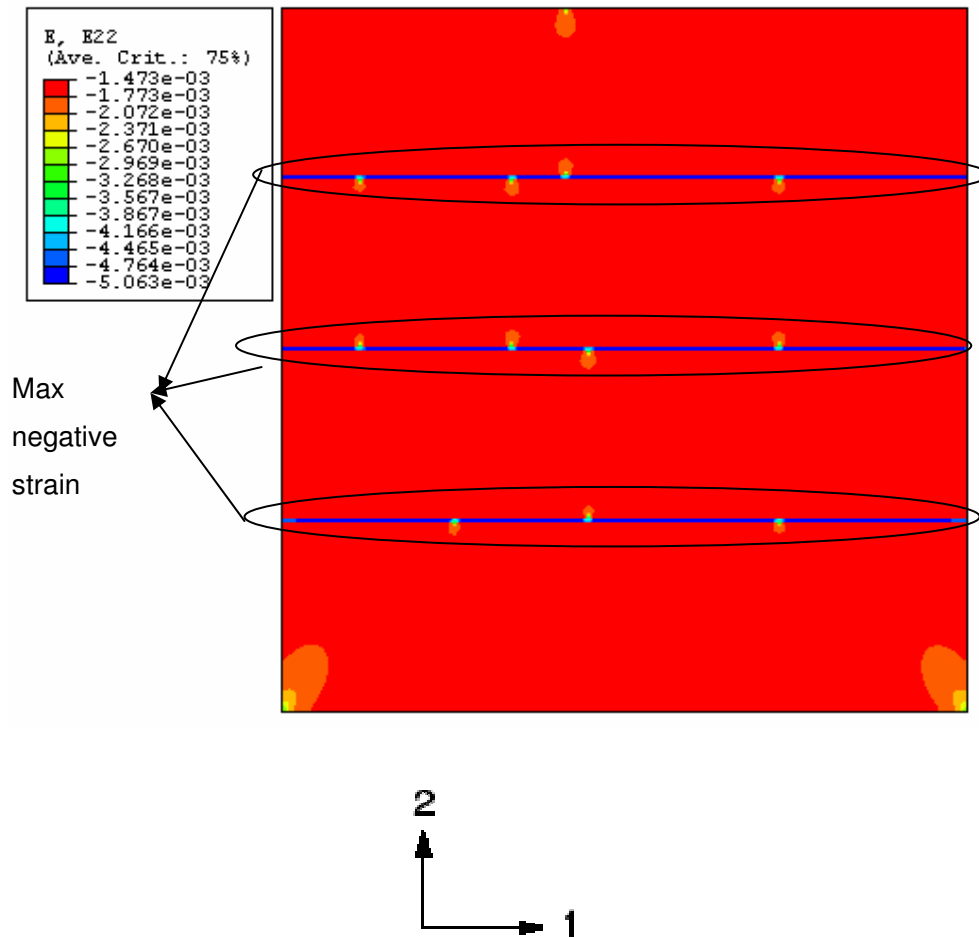


Figure 4.4.1.7 Strain components in 2-2 dir for case B2 panel

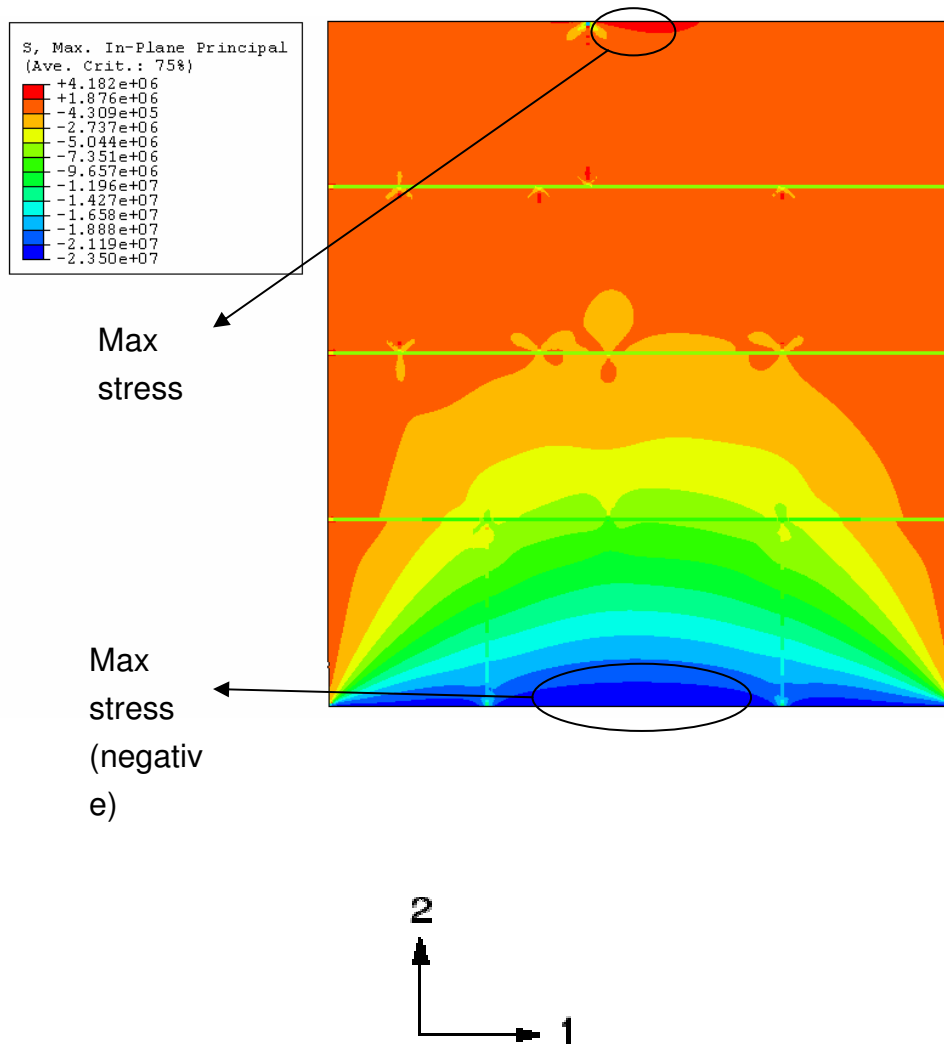


Figure 4.4.1.8 Maximum in plane principal stress for case B2 panel

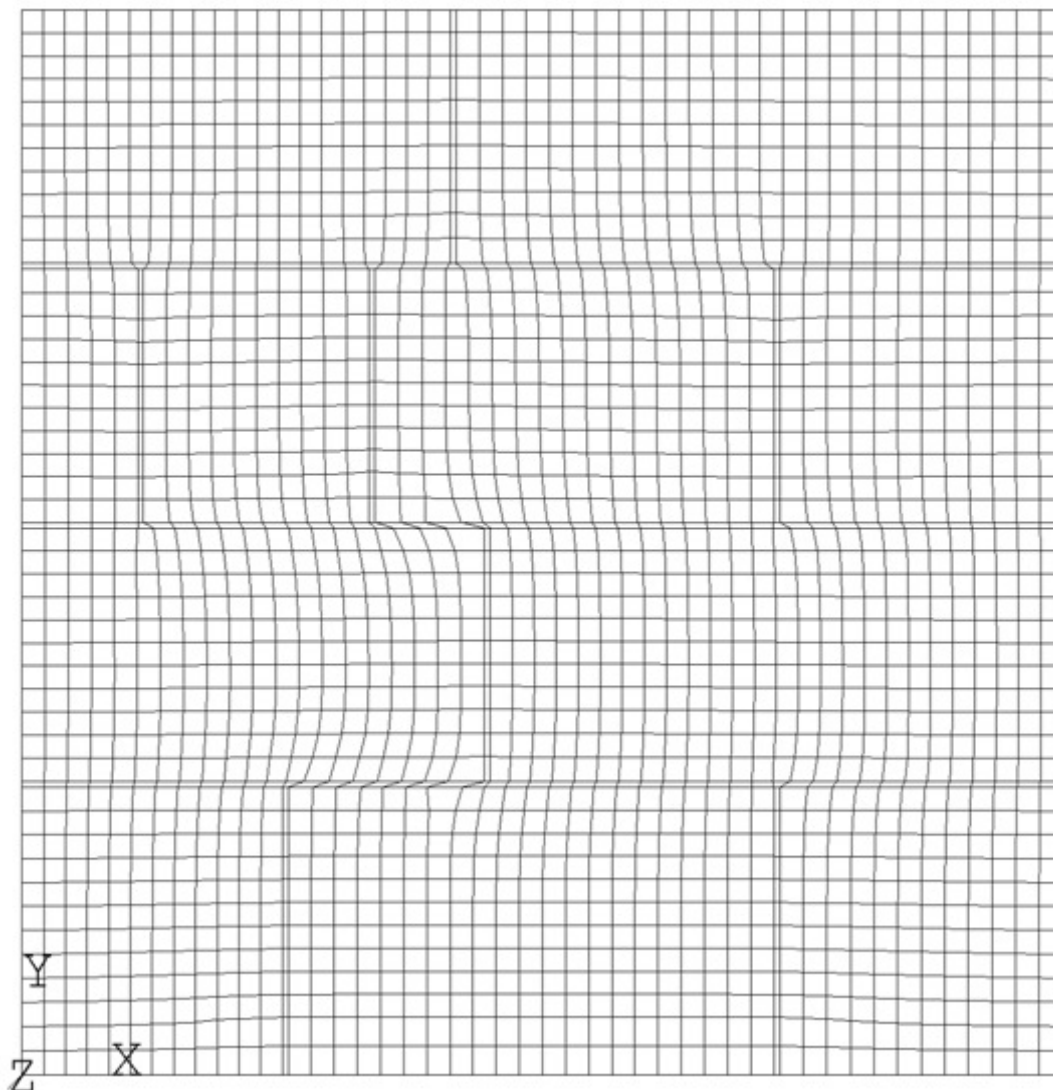


Figure 4.4.2.1 FEM mesh (no. of elements =2256) with approximate global element size of 0.04m

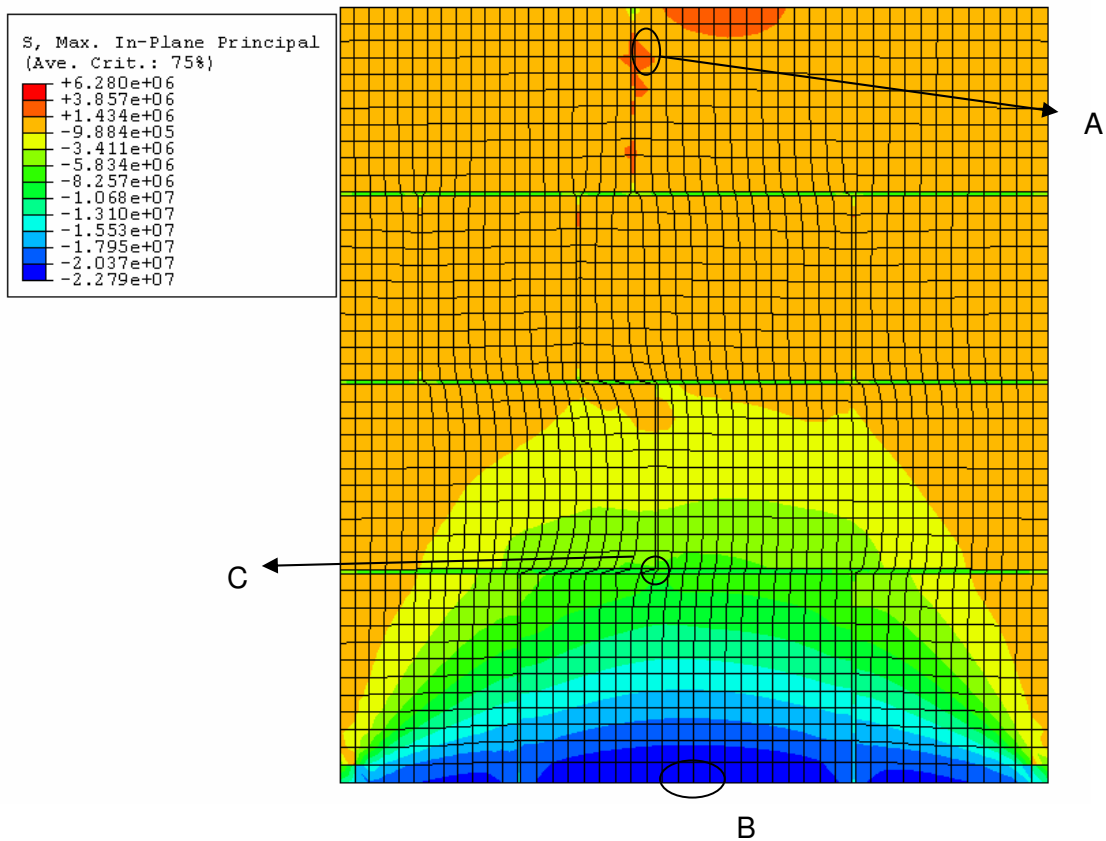


Figure 4.4.2.2 Critical regions selected from the coarse meshed wall panel (no. of elements =2256)

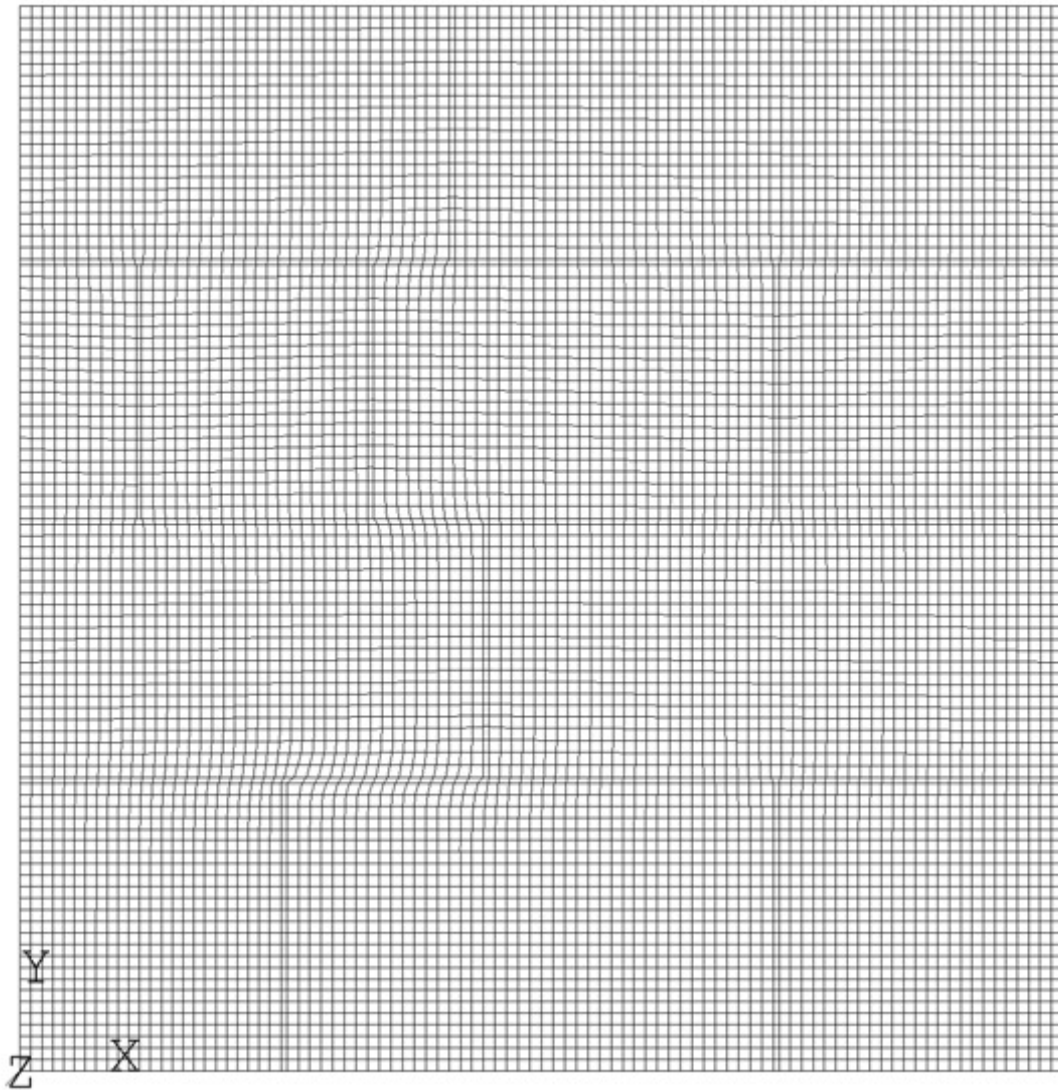


Figure 4.4.2.3 FEM mesh (no. of elements =8742) with approximate global element size of 0.02m.

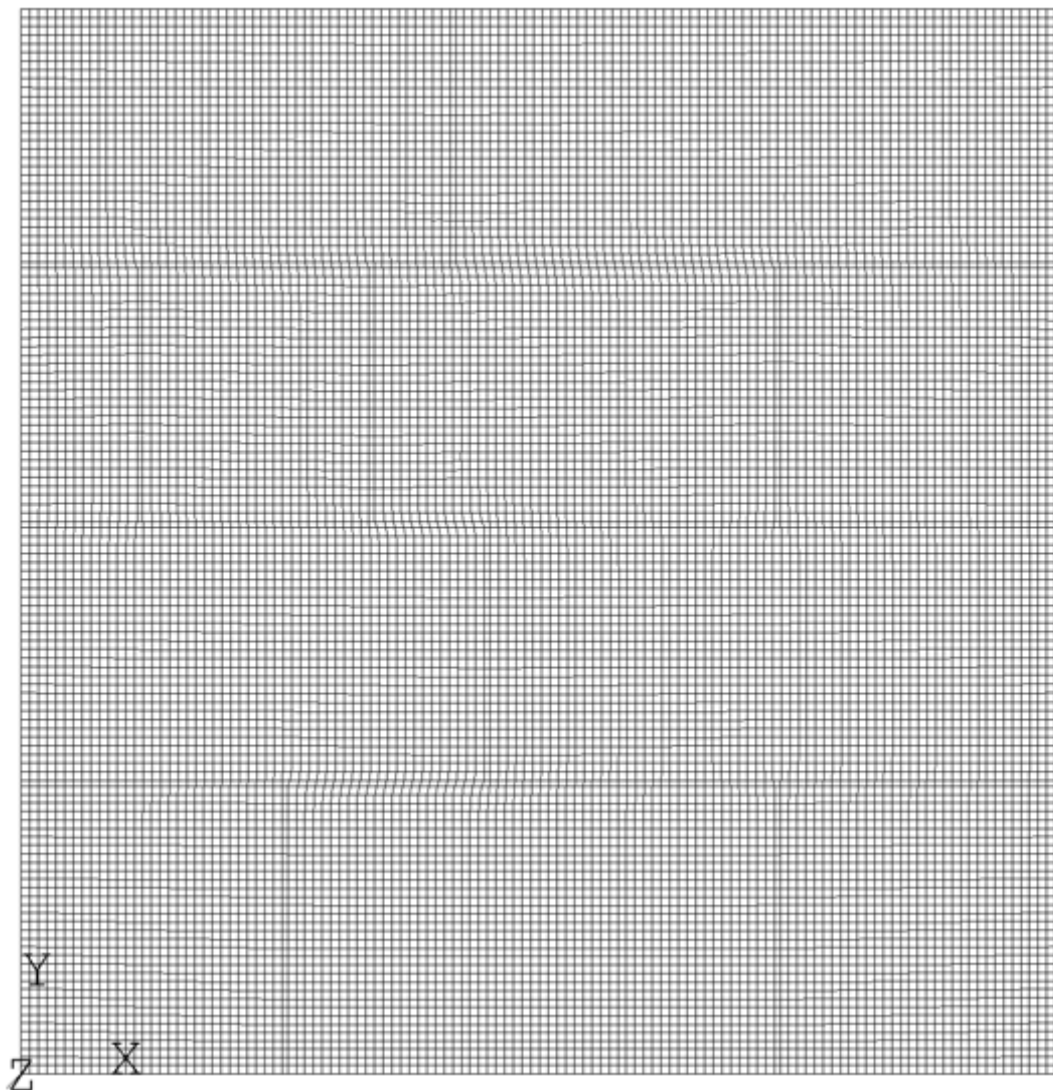


Figure 4.4.2.4 FEM mesh (no. of elements =15004) with approximate global element size of 0.015m.

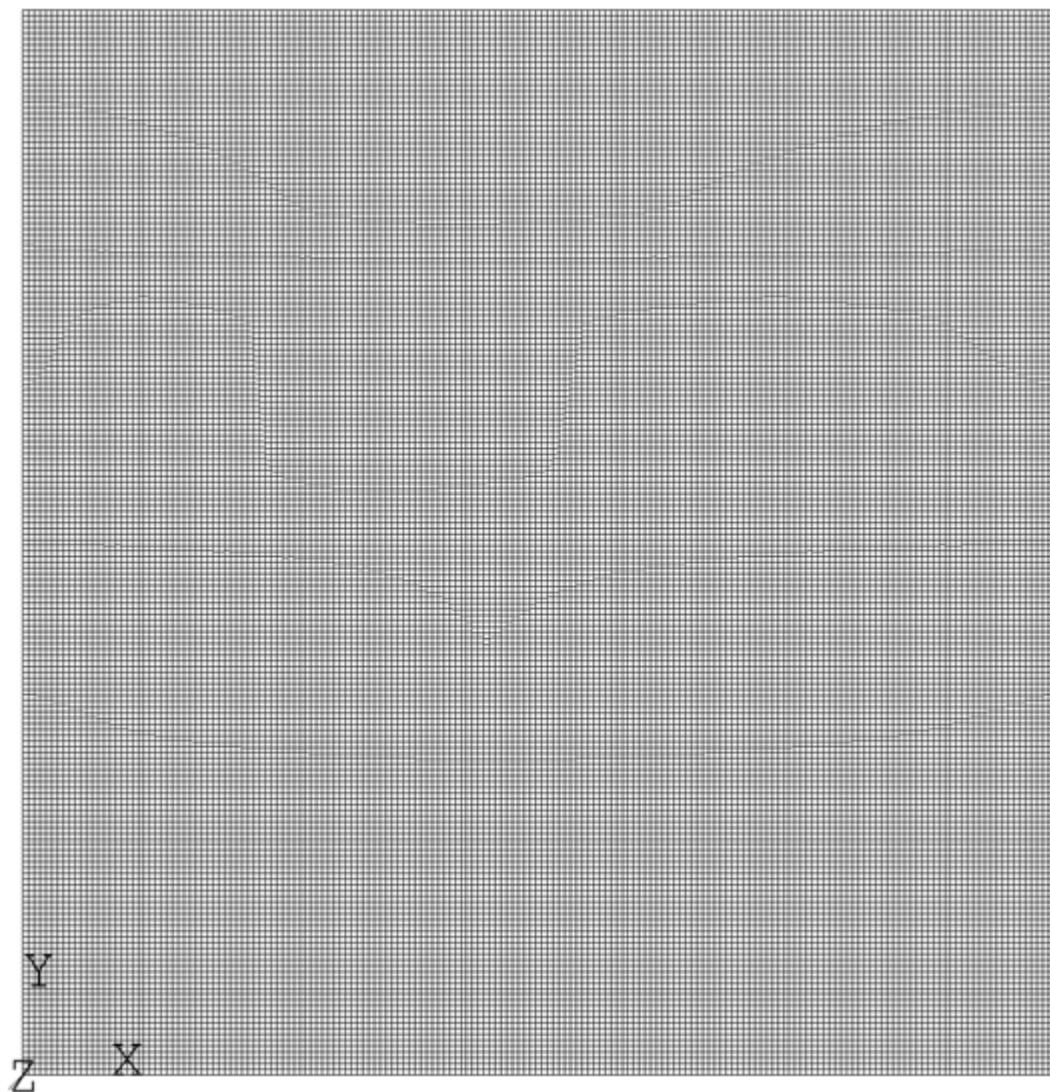


Figure 4.4.2.5 FEM mesh (no. of elements =33300) with approximate global element size of 0.01m.

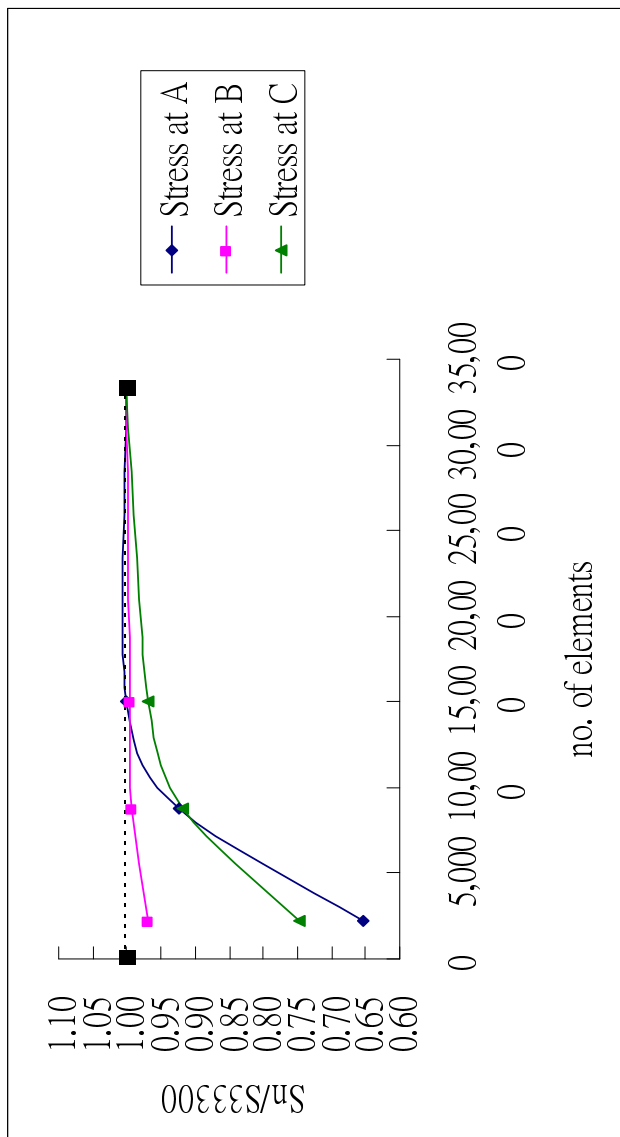


Figure 4.4.2.6 Graph showing the normalized stress vs. no. of elements in the wall panel mesh

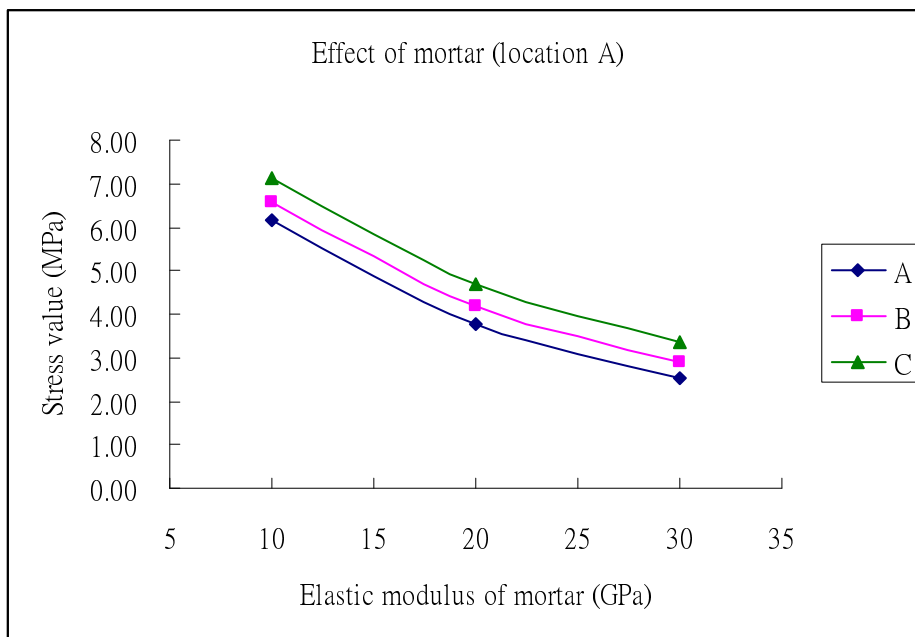


Figure 4.4.3.1 Effects of the stress value at location A in varying the elastic of mortar for case A, b and C.

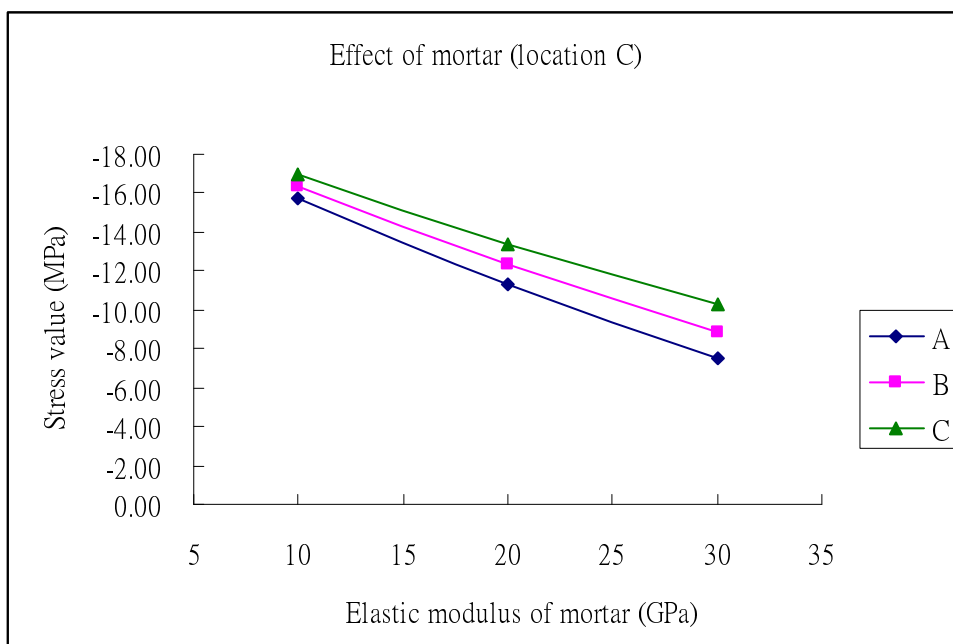


Figure 4.4.3.2 Effects of the stress value at location C in varying the elastic of mortar for case A,B and C.

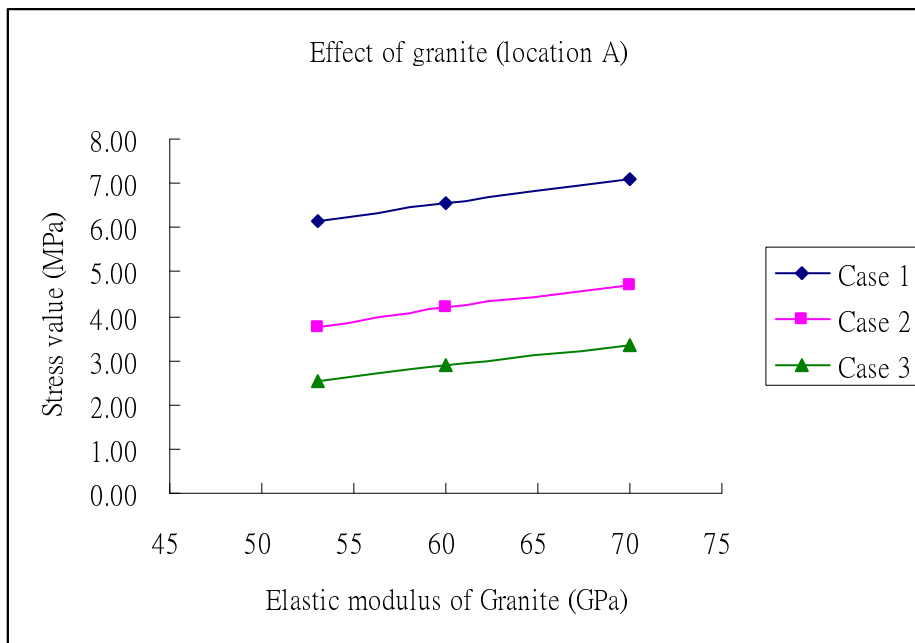


Figure 4.4.3.3 Effects of the stress value at location A in varying the elastic of granite for case A, B and C.

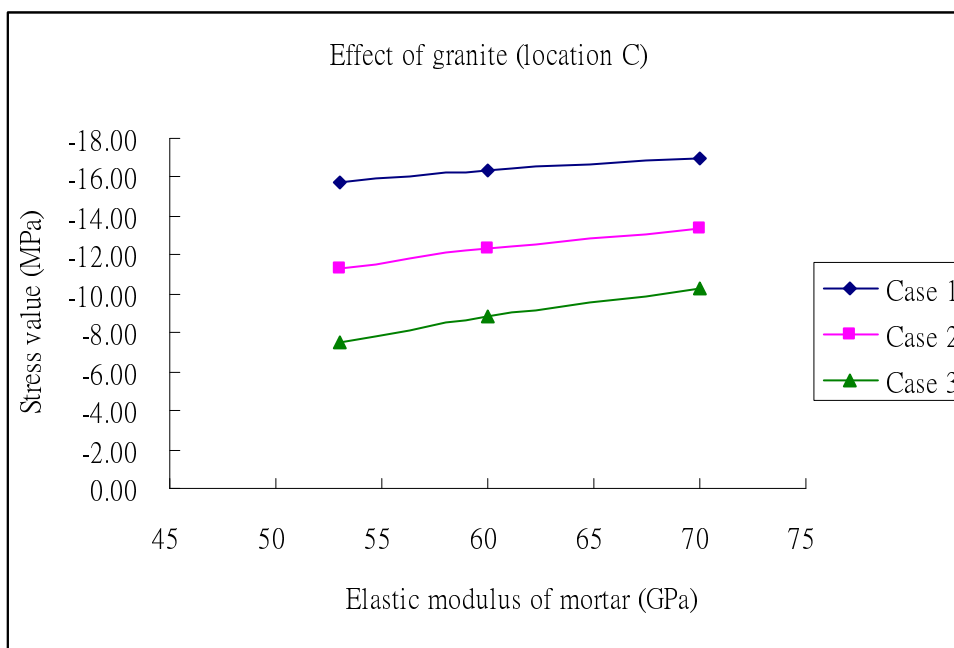


Figure 4.4.3.4 Effects of the stress value at location C in varying the elastic of granite for case A, B and C.

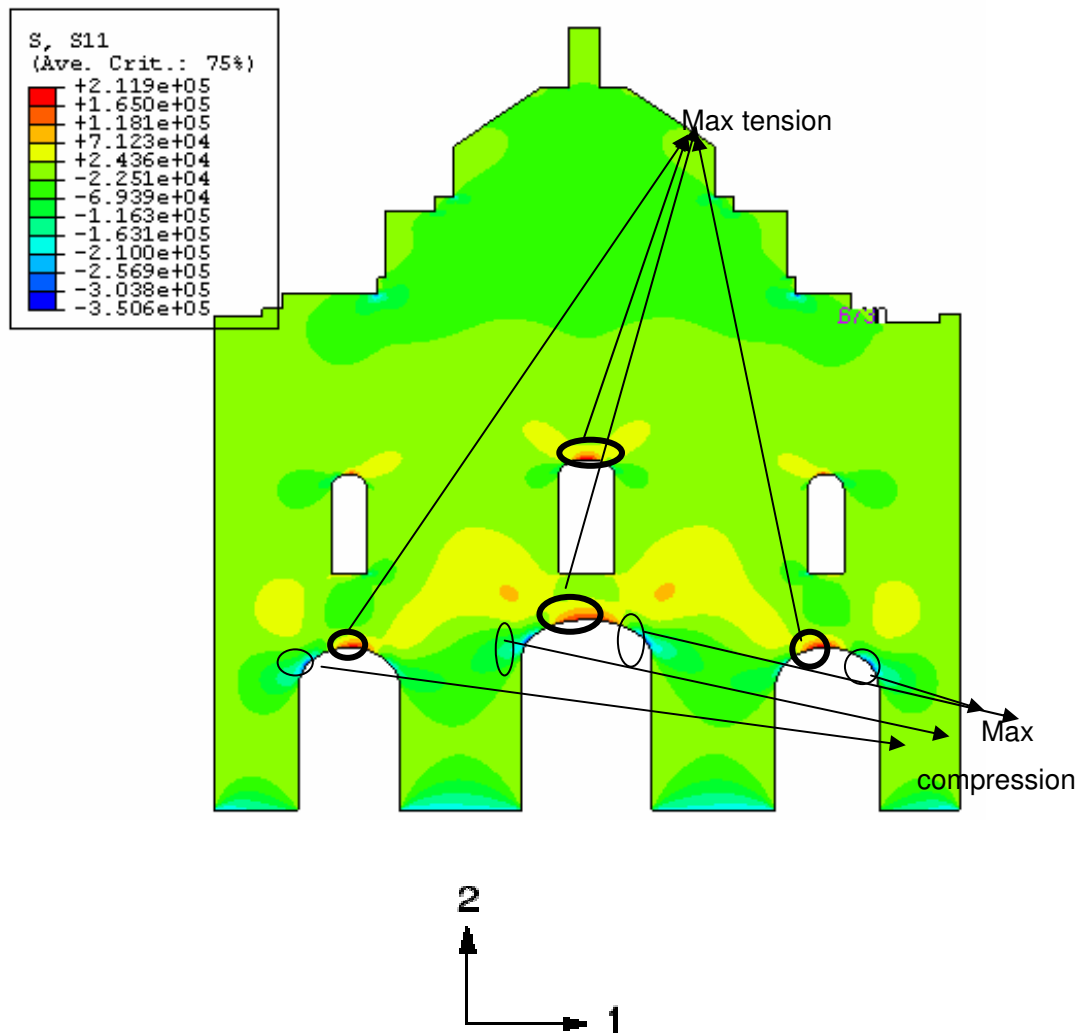


Figure 4.5.1.1 Stress in 1-1 dir distribution contour of the façade

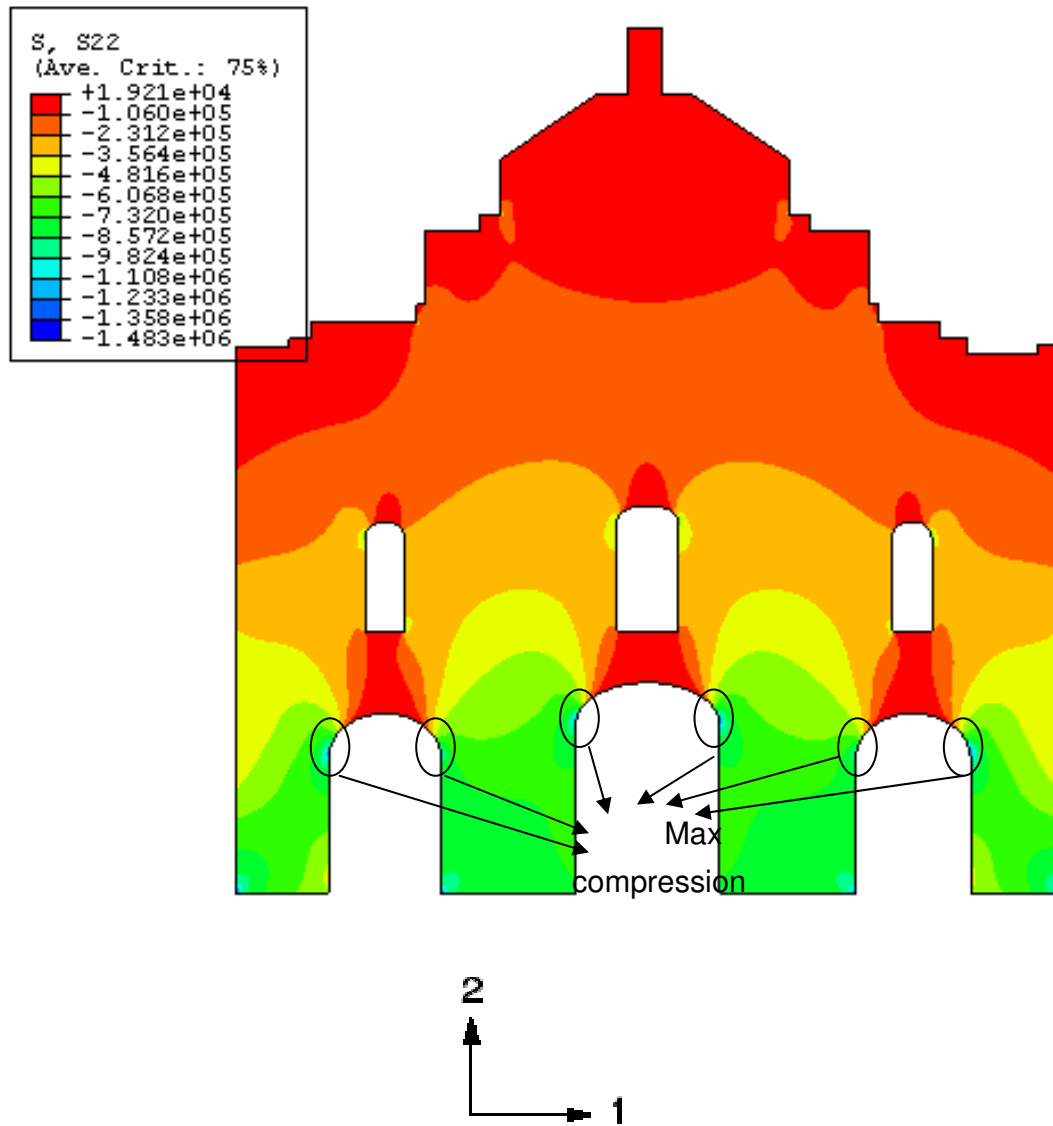


Figure 4.5.1.2 Stress in 2-2 direction distribution contour of the façade

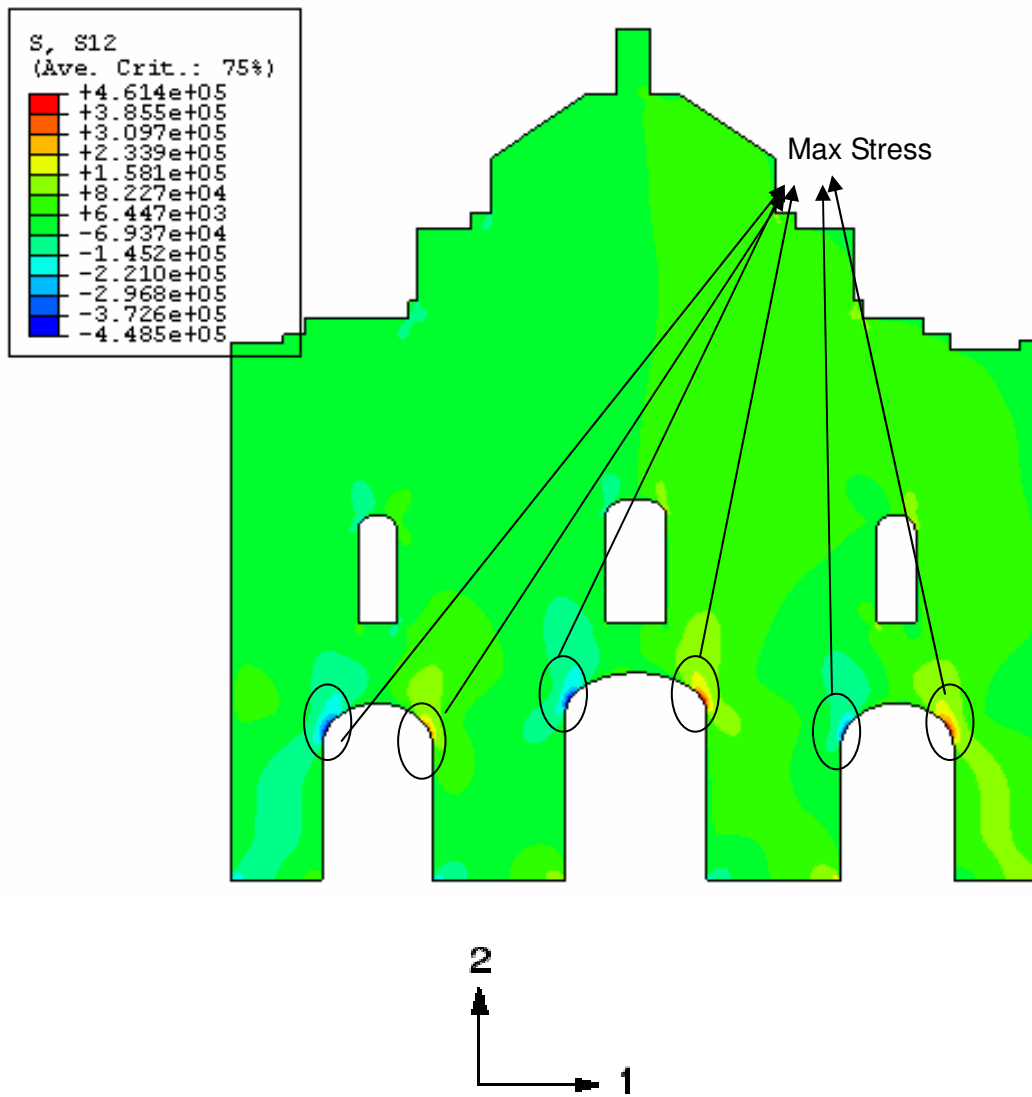


Figure 4.5.1.3 Stress12 distribution contour of the façade

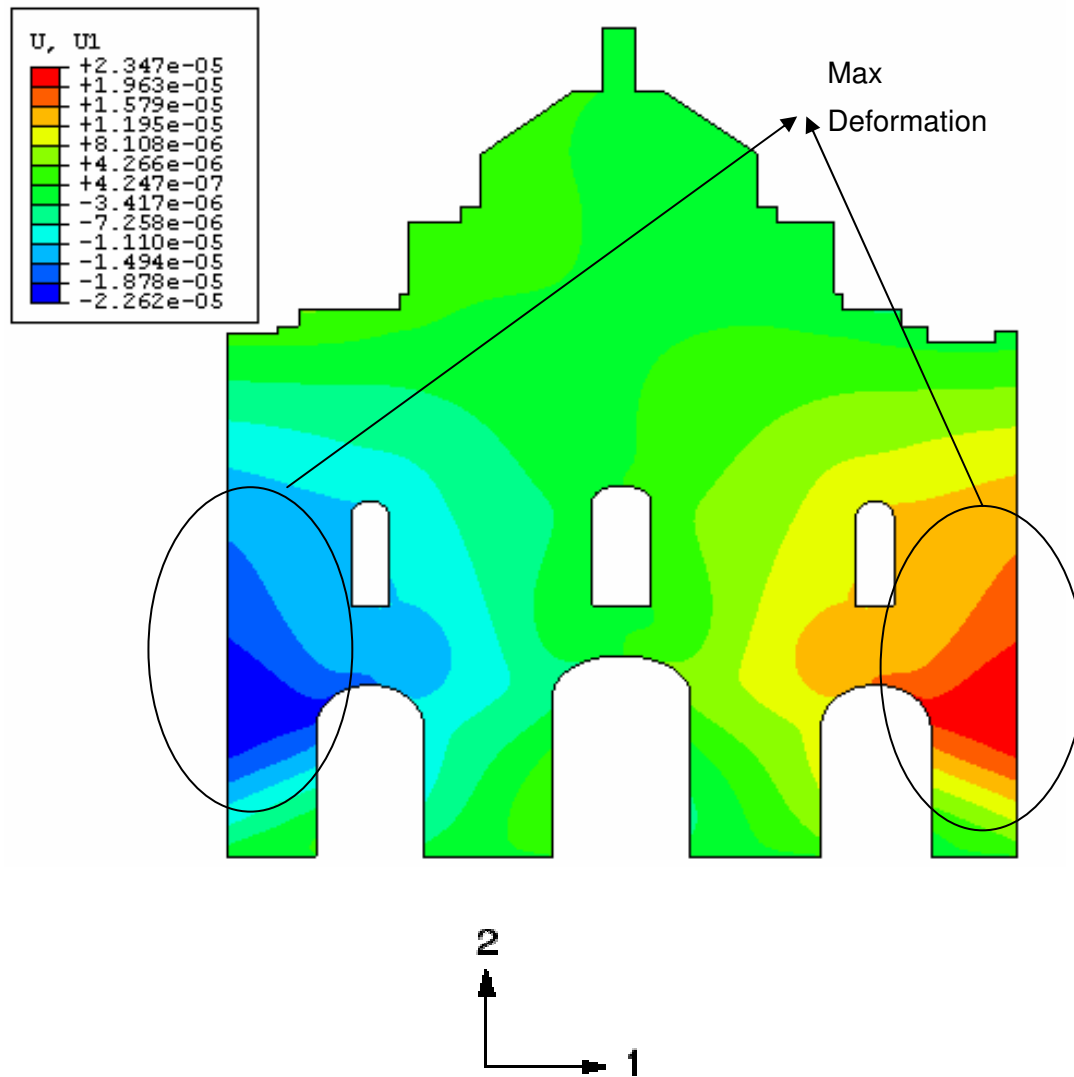


Figure 4.5.1.4 Displacement in 1-1 direction contour of the façade

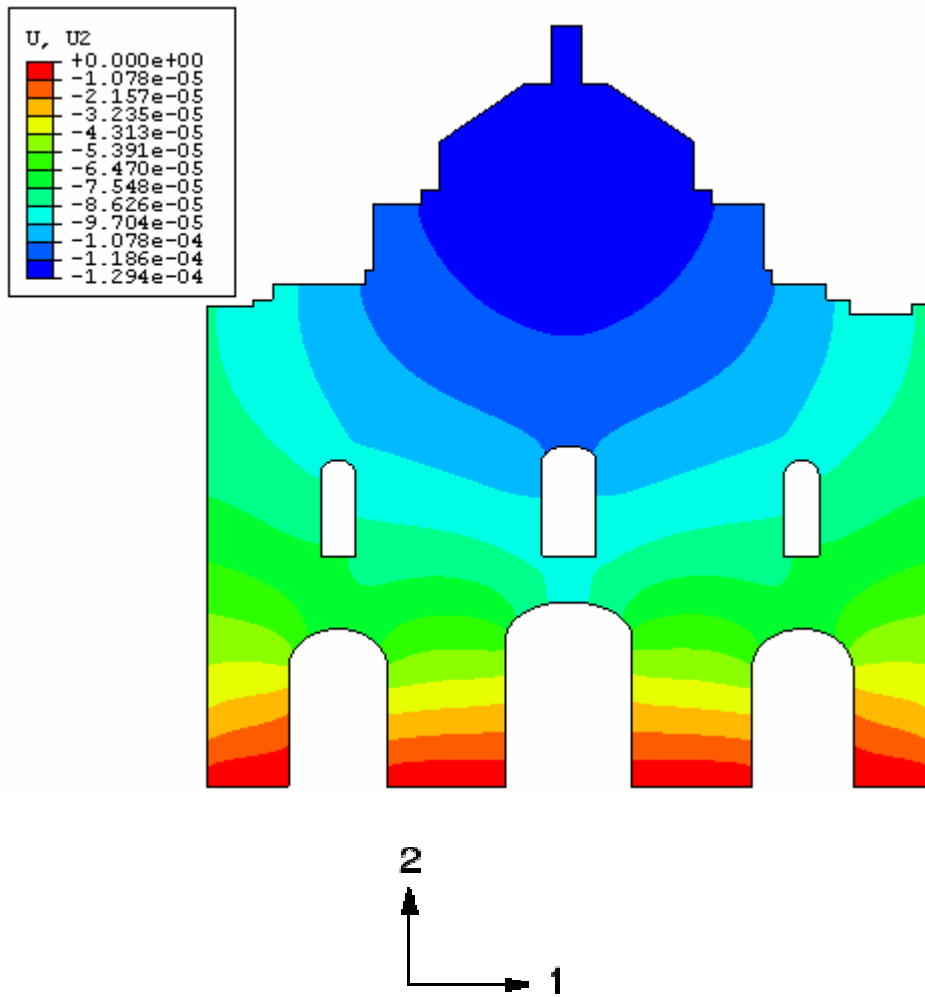


Figure 4.5.1.5 Displacement in 2-2 direction contour of the façade

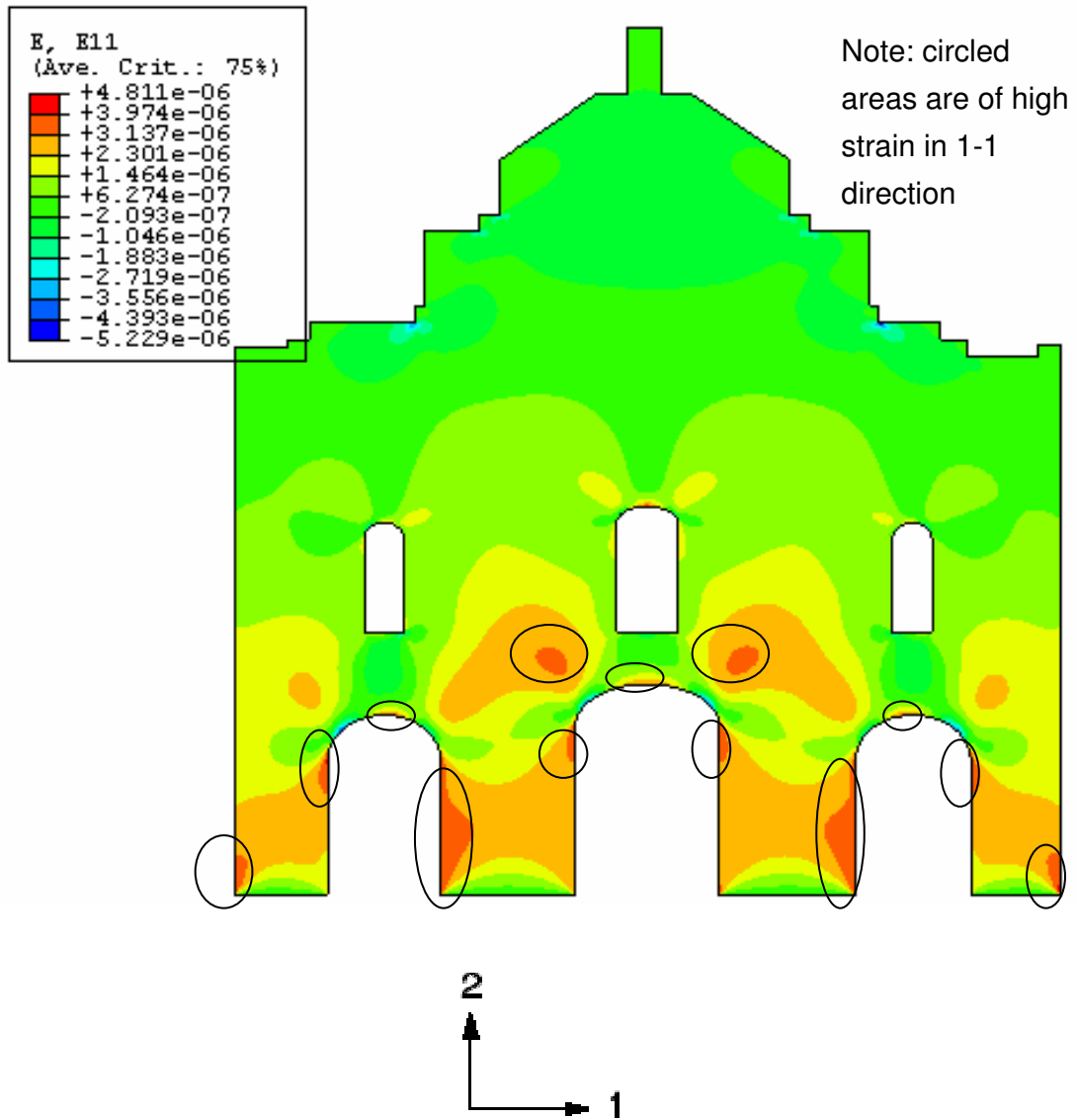


Figure 4.5.1.6 Strain components in 1-1 direction contour of the façade

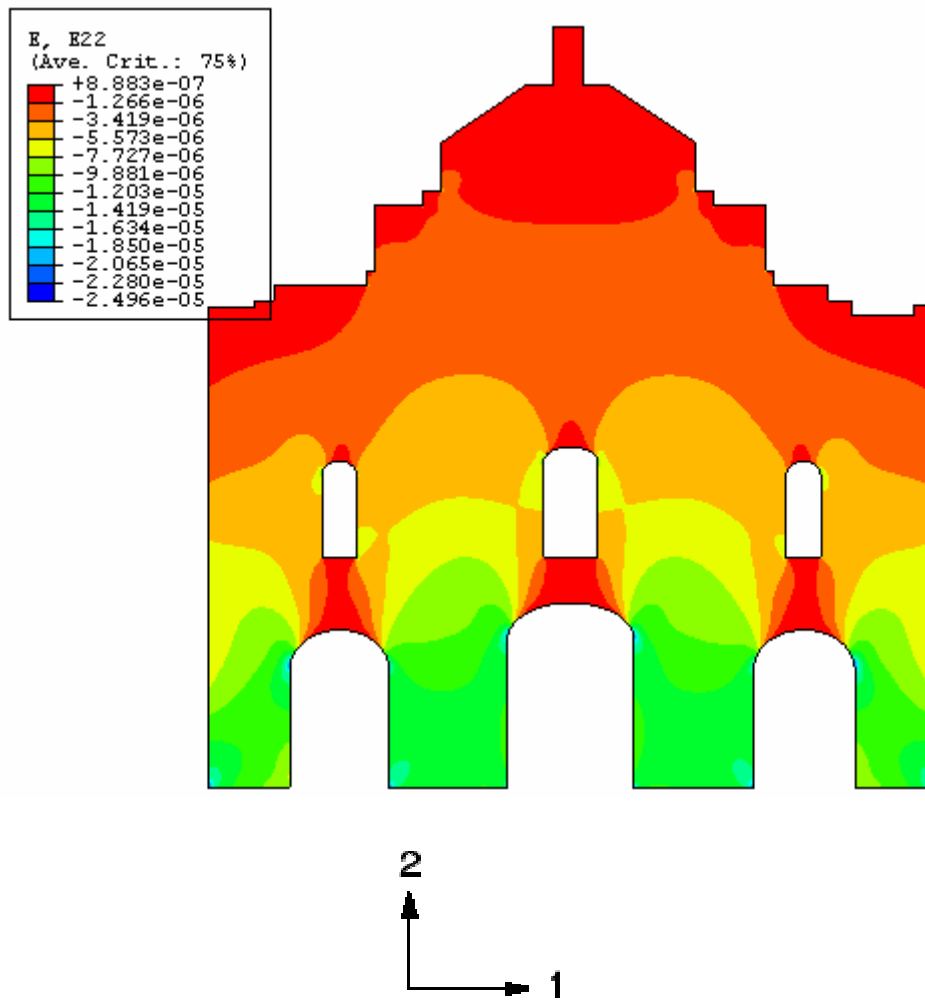


Figure 4.5.1.7 Strain components in 2-2 direction contour of the façade

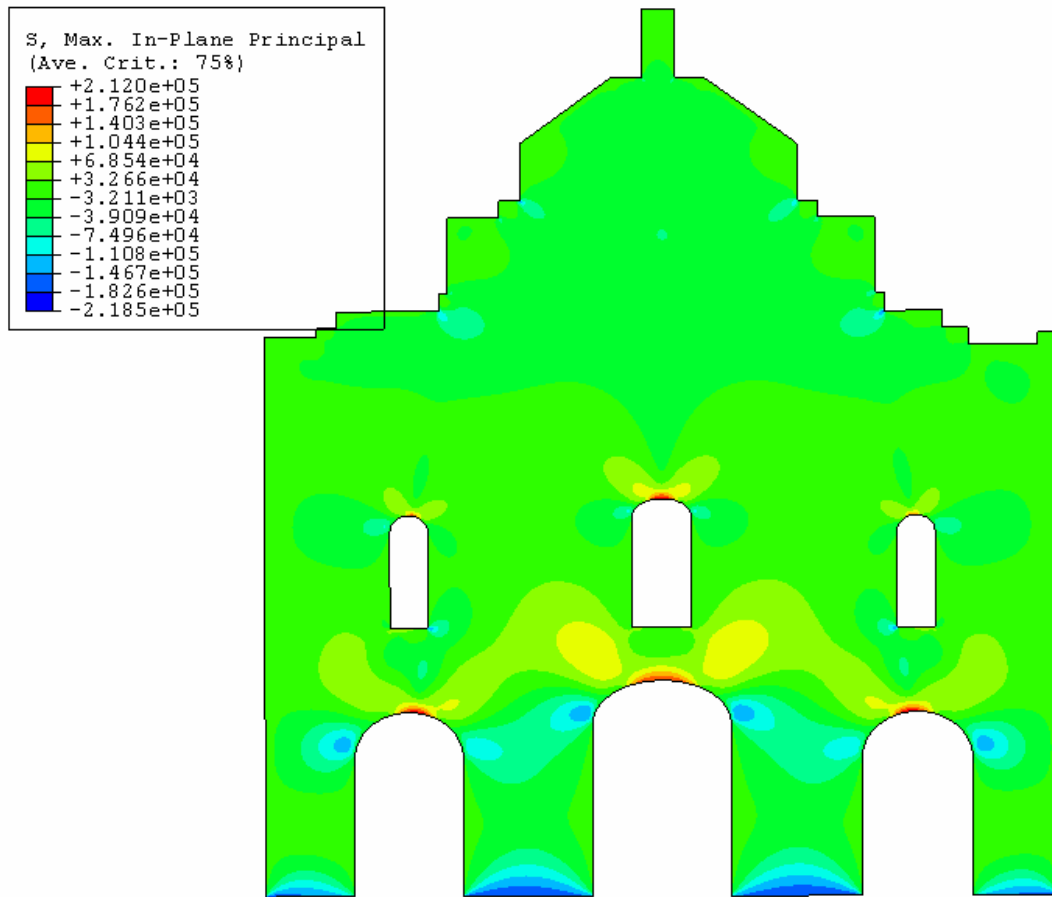


Figure 4.5.1.8 Maximum in plane principal stress of the plane.

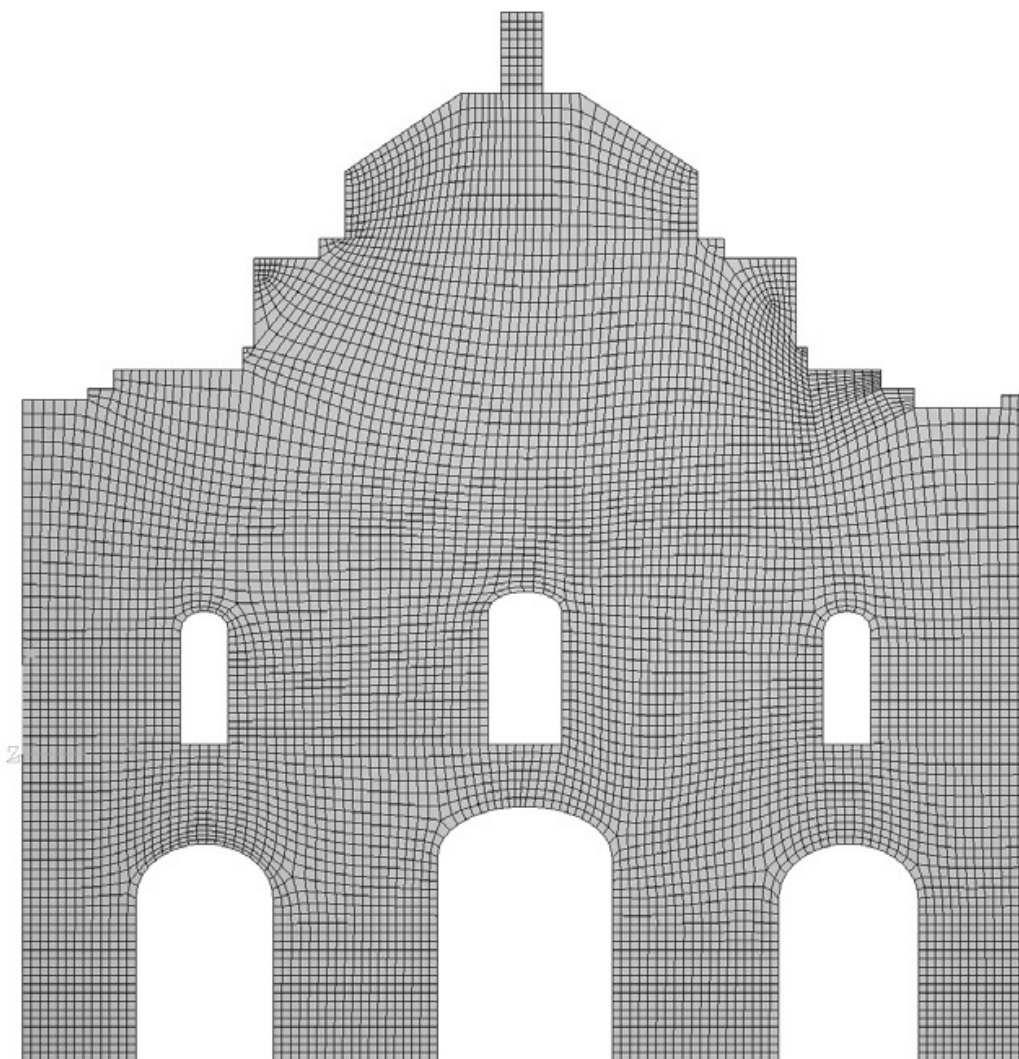


Figure 4.5.2.1 FEM mesh of the façade (no. of elements =7659).

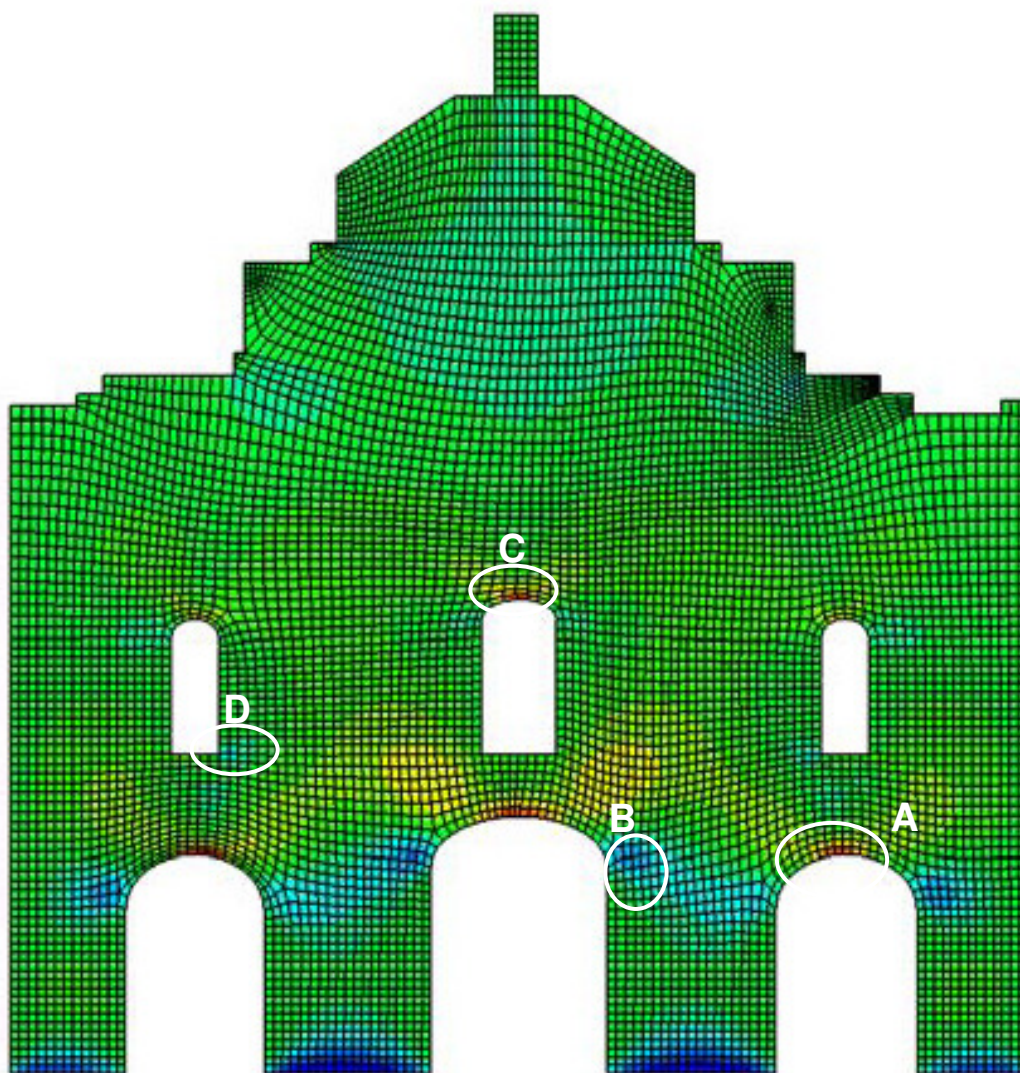


Figure 4.5.2.2 Interest locations in the FEM of the façade (no. of elements =7659).

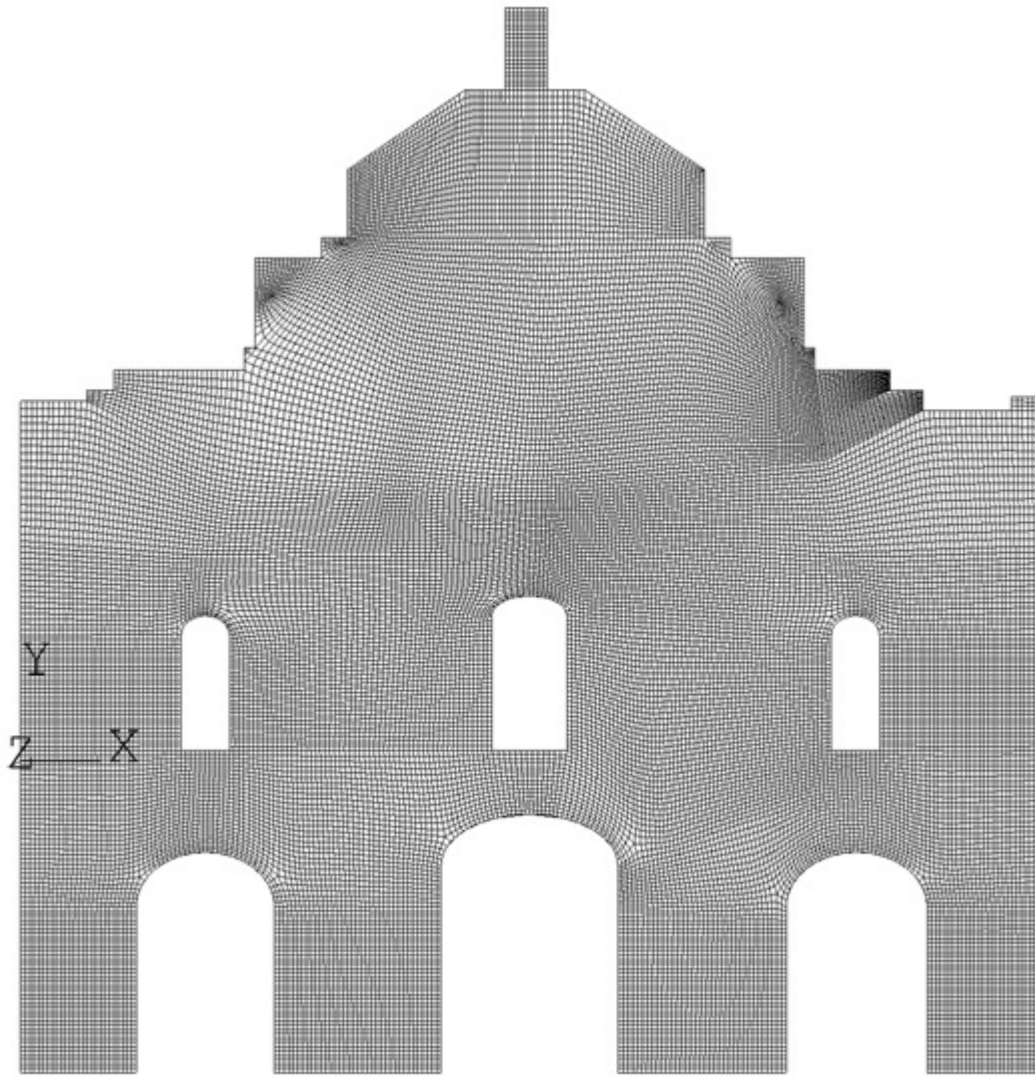


Figure 4.5.2.3 FEM mesh of the façade (no. of elements =30991) with approximate global element size of 0.1m.

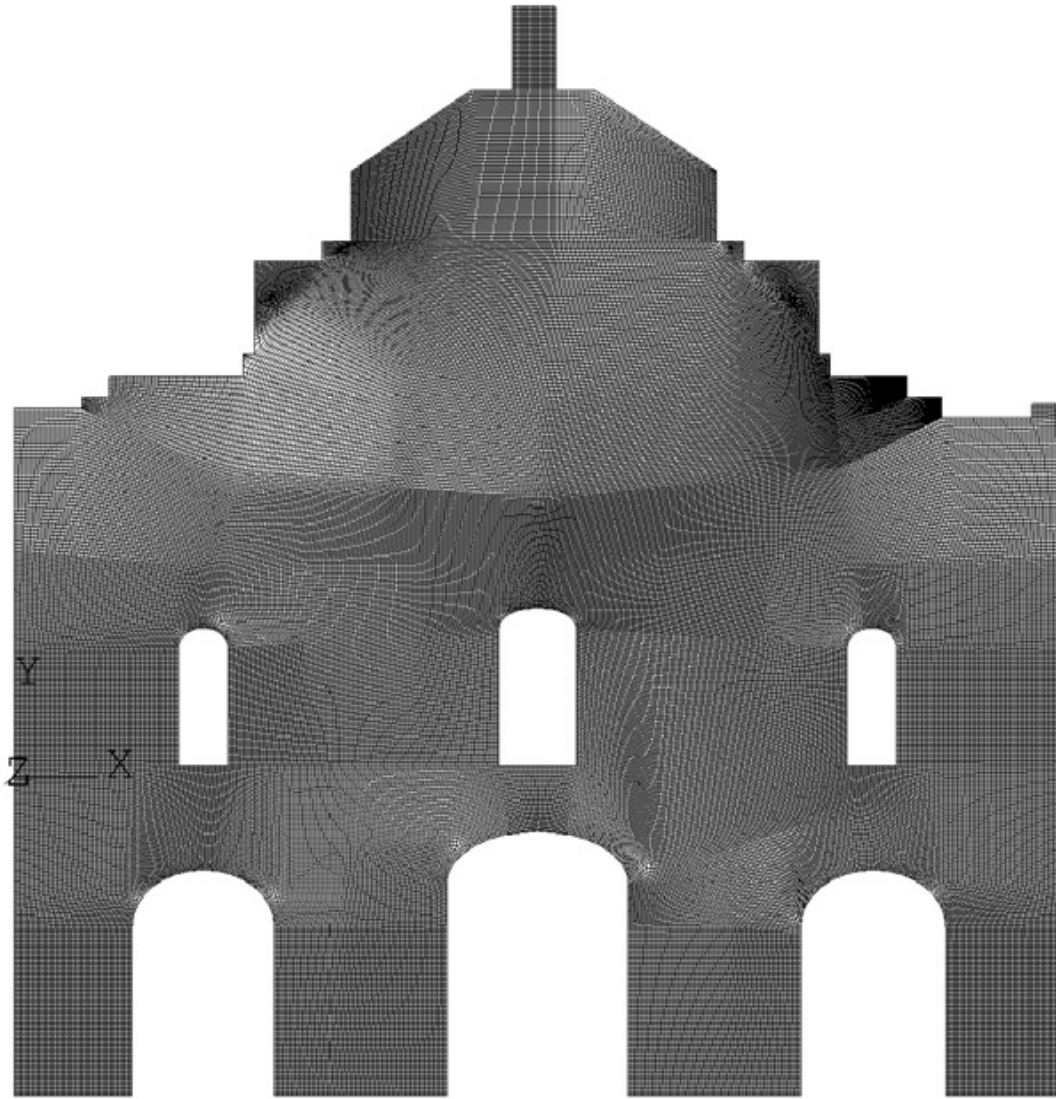


Figure 4.5.2.4 FEM mesh of the façade (no. of elements =122384) with approximate global element size of 0.05m.

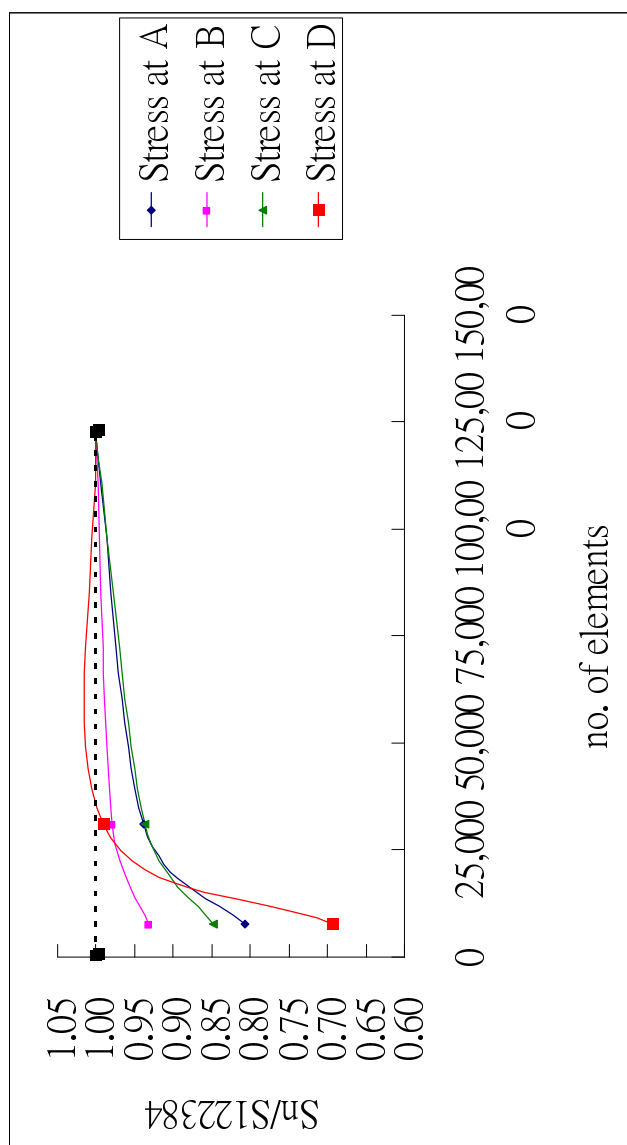


Figure 4.5.2.5 Graph showing the normalized stress vs. the number of elements in the façade's mesh.

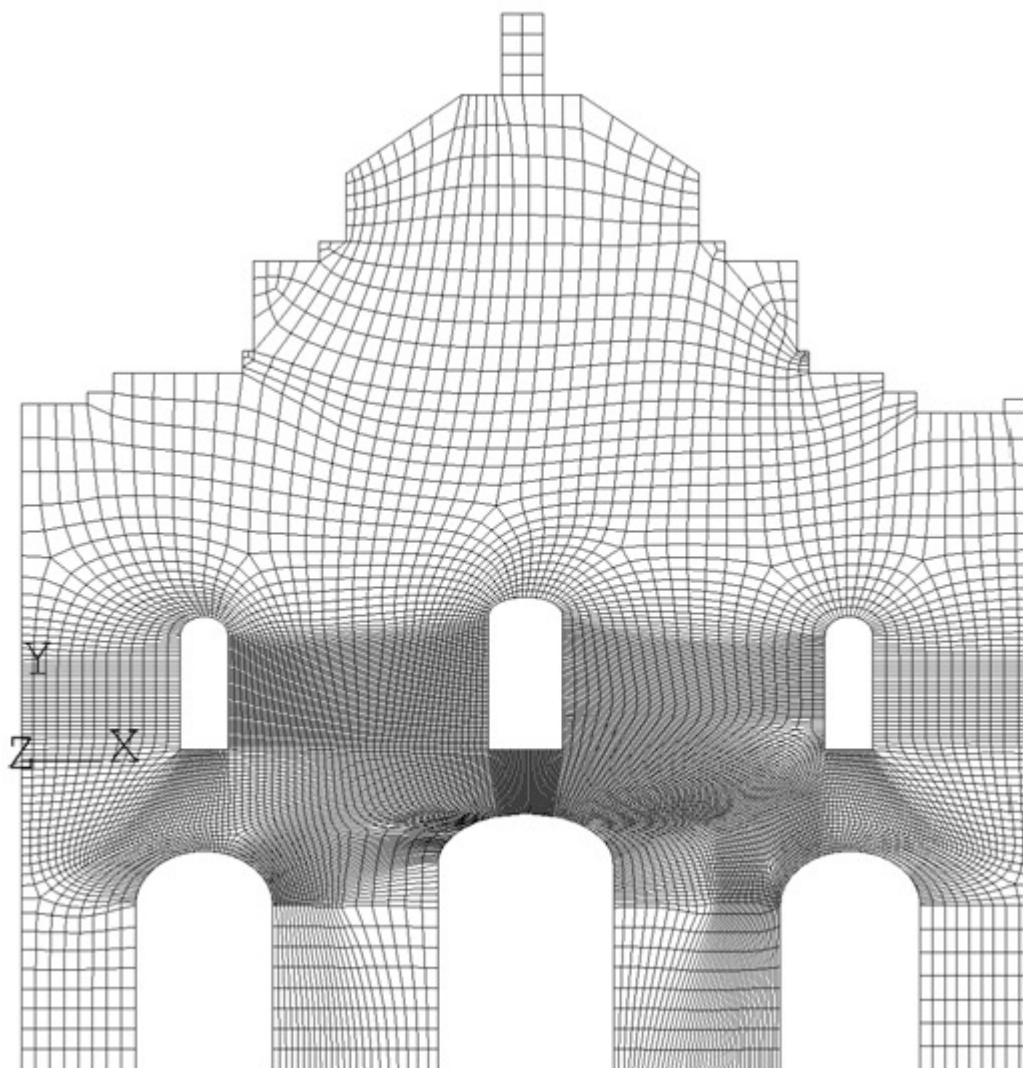


Figure 4.5.2.6 FEM mesh of the façade (no. of elements =13617).

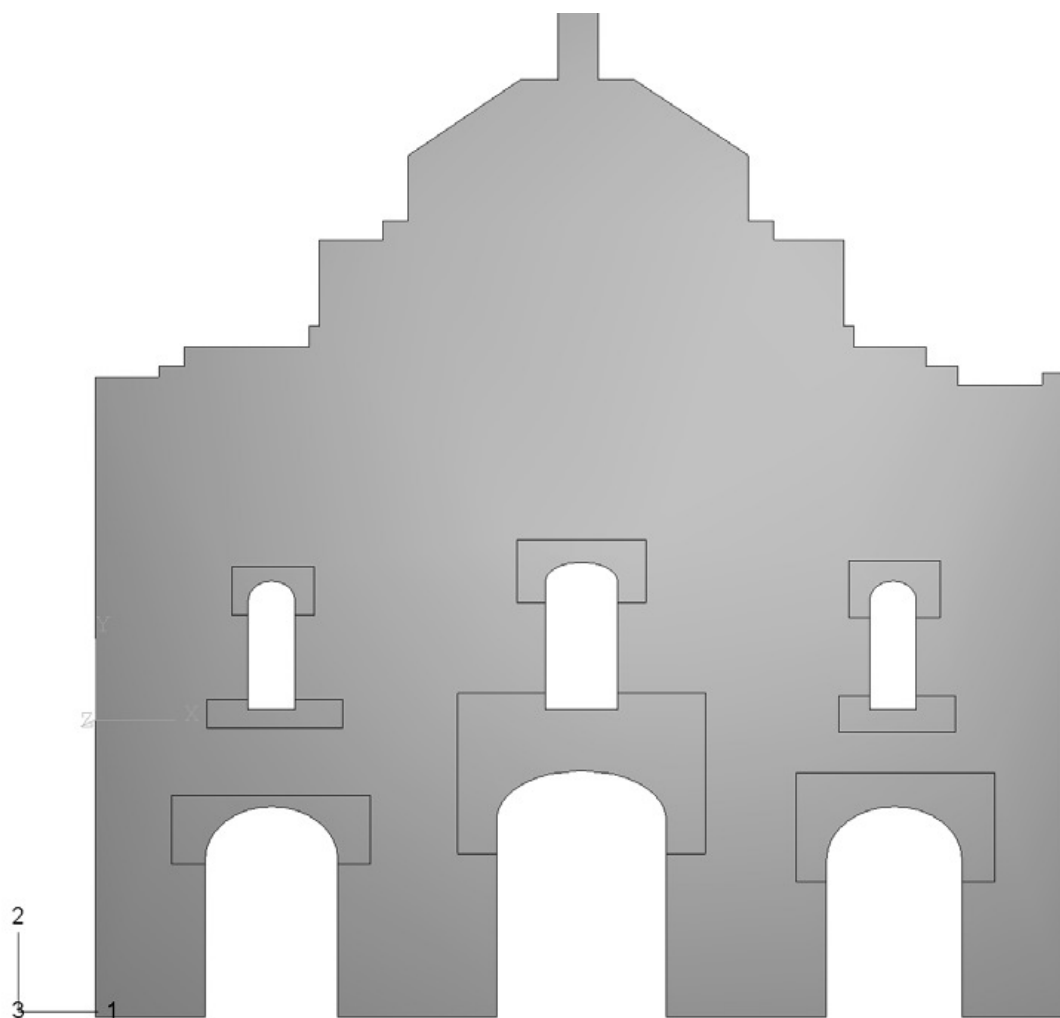


Figure 4.5.2.7 Locations seeded with smaller size.

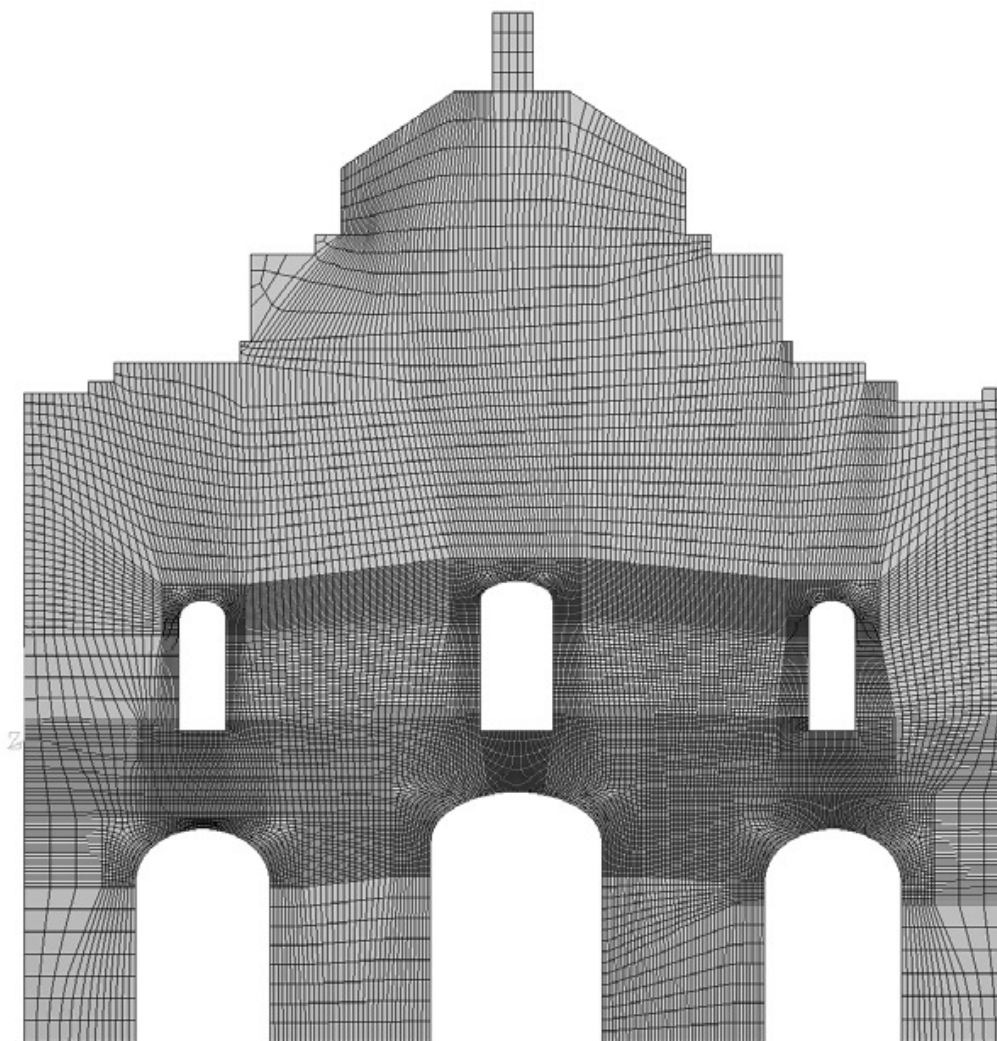


Figure 4.5.2.8 FEM mesh of the façade (no. of elements =24565).

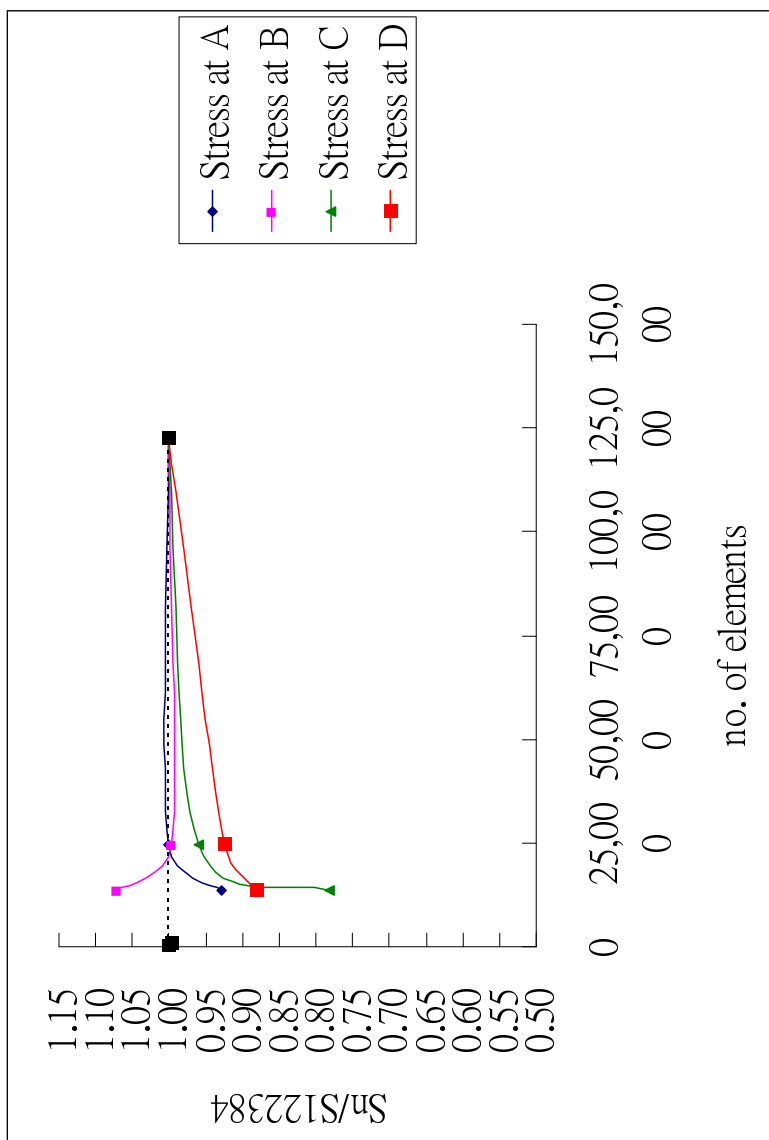


Figure 4.5.2.9 Graph showing the normalized stress vs. the number of elements of the façade's mesh. (finer meshes at critical regions)

## CHAPTER 5 CONCLUSIONS

The following conclusions can be drawn

- The most common type of architecture heritage is masonry structure. Computational modeling of historic masonry structure requires specific strategies. The numerical tools for modeling masonry have been reviewed. It is found that macro-modeling is simple and good enough for preliminary analysis for the current structure in question.
- A parametric stress analysis of façade of the Ruins of St Paul's in Macau has been carried out. The adopted modeling approach is based on the uncoupled homogenization strategy, where the effective elastic properties are first estimated using an engineering homogenization technique followed by a macroscopic two-dimensional analysis of the structure. This approach is conceptually simple.
- Linear elastic analysis has been carried out for macroscopic modeling. Mesh study shows that the total number of elements of around 25,000 is good enough for the type of ruin structure. Moreover, the maximum in plane principal stress of façade, due to self weight, ranges from 0.21 MPa (tension) to -0.22 MPa (compression). Critical points regarding high compressive and tensile stress are located. This finding is consistent with some existing locations, in which strengthening has been carried out in the facade.



## REFERENCES

- Anthoine A. (1995) "Derivation of the in-plane elastic characteristics of masonry through homogenization theory", *Int. J. Solids Structures*, 32(2), 137 – 163.
- Cecchi A. and Di Marco R. (2000), "Homogenization of masonry walls with a computational oriented procedure. Rigid or elastic block?", *Euro. J. of Mech. A/Solids*, 19, 535 – 546.
- Cecchi A. and Sab K (2002) "A multi parameter homogenization study for modeling elastic masonry", *Euro. J. of Mech. A/Solids*, 21, 249 – 268.
- De Borst R. and Feenstra, P.H. (1990) "Studies in anisotropic plasticity with reference to the Hill criterion", *Int. J. Numer. Methods Engrg.*, 29, 315 – 336.
- Giambanco, G. and Rizzo, S. and Spallino, R.(2001) "Numerical analysis of masonry structures via interface model", *Comput. Method. Appl. M.*, 190, 6493 - 6511.
- Hart, V.R., Cundall, P. and Lemos, J. (1998) "Formulation of a three-dimensional distinct element model – Part ii: Mechanical calculations for motions and interaction of a system composed of many polyhedral blocks", *Int. J. Rock. Mech. Min.*, 25, 117 – 126.
- Hill, R. (1948) "A theory of the yielding and plastic flow of anisotropic metals", *Proc. Roy. Soc., (London) A*, 193, 281 – 288.
- Hoffman, O. (1967) "The brittle strength of orthotropic materials", *J. Composite Mat.*, 1, 200 -206.
- Hordijk, D.A. (1991) Local approach to fatigue, PhD Dissertation, Delft University of Technology, Delft, The Netherlands
- Lourenco, P. B., de Borst, R. and Rots, J.G. (1997) "A plane stress softening plasticity model for orthotropic materials", *Int. J. Numer. Meth. Eng.*, 40(21), 4033 – 4057.
- Lourenco, P.B. (1996) Computational strategies for masonry structures, PhD Thesis, Delft University of Technology, Delft, The Netherlands
- Lourenco, P.B. (2002) "Computations on historic masonry structures", *Progress in Advanced Master in Structural Analysis of Monuments and Historical Constructions*

*Structural Engineering and Materials*, 4(3), 301 – 319.

Lourenco, P.B. and Rots, J.G. (1997) “A multi-surface interface model for the analysis of masonry structures”, *J. Eng. Mech – ASCE*, 123(7), 660 – 668.

Mistler M., Anthoine A. and Butenweg C (2007) “In-plane and out-of plane homogenization of masonry”, *Computational Structures Technology*, Vol. 85, Issue 17-18, 1321 – 1330.

Mohamad, G., Lourenco, P.B.& Roman, H.R. (2006) “Poisson behaviour of bedding mortar under multiaxial stress state”, In: 7<sup>th</sup> International Masonry Conference, London.

Pande, G.N., Liang J.X. and Middleton J. (1989) “Equivalent elastic moduli for brick masonry”, *Comput. Geotech.*, 8, 243 – 265.

Papa, E. (1990) About damage mechanics with particular reference to masonry (in Italian), Dissertation, Politecnico di Milano, Milan, Italy.

Papa, E. and Nappi, A. (1997) “Numerical modeling of masonry: a material model accounting for damage effects and plastic strains”, *Applied Mathematics Modeling*, 21, 319 – 335.

Pietruszczak, S and Niu, X. (1992) “A mathematical description of macroscopic behaviour of brick masonry”, *Int. J. Solids Structures*, 29(5), 531 -546.

Schellekens, J. and De Borst R. (1990) “The use of the Hoffman yield criterion in finite element analysis of anisotropic composites” *Comp. Struct.*, 37(6), 1087 – 1096.

Sejnoha, J., Sejnoha, M., Zeman, J., Sykora, J. and Vorel, J. (2008) “ Mesoscopic study on historic masonry”, <http://en.scientificcommons.org/> , 2008.

Tsai S.W. and Wu, E.M. (1971) “A general theory of strength of anisotropic materials”, *J. Composite Mat.*, 5, 58 -80.

Vonk, R.A. (1992) Softening of concrete loaded in compression, PhD Dissertation, Eindhoven University of Technology, Eindhoven, The Netherlands

Yurdas, I., Burlion, N. and Skoczylas, F. (2004) “Experimental characterization of the Advanced Master in Structural Analysis of Monuments and Historical Constructions

drying effect on uniaxial mechanical behaviour of mortar”, *Materials and Structures*, Vol. 37, April, 170 -176.

Zohdi T.I and Wriggers P. (2005) Introduction to computational micromechanics, Springer-Verlag, Berlin.